
Article:
Frey, A.M., Satur, M.J., Phansopa, C. orcid.org/0000-0003-4943-9228 et al. (7 more authors) (2019) Characterization of Porphyromonas gingivalis sialidase and disruption of its role in host–pathogen interactions. Microbiology, 165 (11). pp. 1181-1197. ISSN 1350-0872

https://doi.org/10.1099/mic.0.000851

Article:
Frey, A.M., Satur, M.J., Phansopa, C. orcid.org/0000-0003-4943-9228 et al. (7 more authors) (2019) Characterization of Porphyromonas gingivalis sialidase and disruption of its role in host–pathogen interactions. Microbiology. ISSN 1350-0872

https://doi.org/10.1099/mic.0.000851

Characterisation of *Porphyromonas gingivalis* sialidase and disruption of its role in host-pathogen interactions

Andrew M Frey[1,2*], Marianne Satur[1], Chatchawal Phansopa[1], Kiyonobu Honma[3], Paulina A Urbanowicz[5], Daniel Spencer[5], Jonathan Pratten[4], David Bradshaw[4], Ashu Sharma[3*] & Graham P Stafford[1*]

Affiliations

[1] Integrated BioSciences, School of Clinical Dentistry, The University of Sheffield, 19 Claremont Crescent, Sheffield S10 2TA, U.K.
[2] University of South Florida, Department of Cell Biology, Microbiology, and Molecular Biology, 4202 East Fowler Ave, ISA2015, Tampa, FL 33620
[3] Dept. of Oral Biology, University at Buffalo, Buffalo, NY, United States.
[4] Oral Health R&D, GlaxoSmithKline, St. Georges Avenue, Weybridge, KT13 0DE, U.K.
[5] Ludger Ltd., Culham Science Centre, Oxfordshire, OX14 3EB, U.K.
[*] Corresponding authors

Graham Stafford- g.stafford@sheffield.ac.uk, phone: 0044 (114) 2159413
Ashu Sharma- sharmaa@buffalo.edu, phone: 001 (716) 8292759
Andrew Frey- andrewfrey@usf.edu, 001 (813) 9745259

Keywords: Sialidase, host-pathogen interactions, biofilm, glycoprotein, periodontitis, gingivitis

Abstract

Key to onset and progression of periodontitis is a complex relationship between oral bacteria and the host. The organisms most associated with severe periodontitis are the periodontal pathogens of the red complex; *Tannerella forsythia*, *Treponema denticola*, and *Porphyromonas gingivalis*. These organisms express sialidases, which cleave sialic acid from host glycoproteins, and contribute to disease through various mechanisms. Here, we expressed and purified recombinant *P. gingivalis* sialidase SiaPG (PG_0352) and characterised its activity on a number of substrates, including host sialoglycoproteins and highlighting inability to cleave diacetylated sialic acids a phenomenon overcome by the NanS sialate-esterase from *T. forsythia*. Indeed SiaPG required NanS to maximise sialic acid harvesting from heavily O-acetylated substrates such as bovine salivary mucin, hinting at the possibility of interspecies cooperation in sialic acid release from host sources by these members of the oral microbiota. Activity of SiaPG and *P. gingivalis* was inhibited using the commercially available chemotherapeutic zanamivir, indicating its potential as a virulence inhibitor, which also inhibited sialic acid release from mucin, and was capable of inhibiting biofilm formation of *P. gingivalis* on oral glycoprotein sources. Zanamivir also inhibited attachment and invasion of oral

epithelial cells by *P. gingivalis* and other periodontal pathogens, both in monospecies but also in multispecies infection experiments, indicating potential to suppress host-pathogen interactions of a mixed microbial community. This study broadens our understanding of the multifarious roles of bacterial sialidases in virulence, and indicates that their inhibition with chemotherapeutics could be a promising strategy for periodontitis therapy.

Introduction

The black-pigmented, Gram negative, asaccharolytic anaerobe *Porphyromonas gingivalis* has been the focus of much research due to its role in periodontitis where it is often referred to as a "keystone pathogen" [1]. *P. gingivalis* exists as a small part of the microbiome, which sees a population shift to include a greater proportion of certain bacterial species, a state now referred to as dysbiosis [2]. In periodontal disease this population shift was observed in the 1990's, with certain organisms considered particularly important to periodontal disease. *Tannerella forsythia*, *Porphyromonas gingivalis*, and *Treponema denticola* form the so-called red complex which is strongly associated with disease [3], and with the advent of next generation sequencing their presence as a signature of periodontal disease has been well established, along with other organisms which seem to play a causative role in periodontitis [2, 4]. During treatment of periodontitis systemic antibiotics such as azithromycin can be administered as an adjunct to mechanical removal of the subgingival plaque [5]. Despite this a proportion of patients poorly respond to periodontal therapy, and in these patients (post-treatment) the levels of periodontal pathogens are higher than in patients who respond to treatment, or in healthy controls [6]. This difficulty in treatment has led to increased interest in development of an "anti-virulence approach" to target the virulence factors of specific pathogens or groups of pathogens, including those responsible for periodontitis. This has been seen in the case of the gingipains of *P. gingivalis*, with several plant extracts [7, 8], and short peptides [9] shown to reduce gingipain activity, with *in vitro* studies showing reductions in *P. gingivalis* biofilm formation [8], and disruption of bacterial nutrient acquisition leading to decreased *P. gingivalis* growth [9]. Plant extracts that inhibit gingipains have also shown disruption of host-*P. gingivalis* interactions; attachment and invasion of host cells, and cytokine production [7]. Moreover, a recent study showed that treatment with a potent small molecule gingipain inhibitor in mice reduced *P. gingivalis* infection in the brain and further blocked $A\beta_{1\text{-}42}$ production and neurodegenerative Alzheimer disease pathology [10].

Another virulence factor of periodontal pathogens including *P. gingivalis* are sialidases (also called neuraminidases), enzymes frequently expressed by host-dwelling organisms which cleave terminal sialic acid-a family of 9-carbon sugars-from host sialoglycans. In humans the most common sialic acid is N-acetylneuraminic acid (Neu5Ac), and is usually linked by its second carbon to the third or sixth carbon of the underlying sugar (α2-3 or α2-6 linked sialic acid). Sialidases are well established virulence factors in the gut and nasopharyngeal pathogens *Vibrio cholerae* and *Streptococcus pneumoniae*, where they contribute to colonisation, persistence, and ultimately disease [11, 12]. Interestingly, all three periodontal red complex pathogens express a sialidase; PG_0352 (termed SiaPG here) in *P. gingivalis*, NanH in *T. forsythia*, and TDE0471 in *T. denticola*. Other periodontal

pathogens also possess mechanisms to process sialic acid in the absence of sialidase expression, such as some *Fusobacterium nucleatum spp.*, which possess neuraminate lyase for catabolism of sialic acid [13]. It is thought that acquisition of sialic acid by organisms that do not possess sialidases is due to the overall action of the microbial community of which they are part of. Additionally, periodontal organisms tentatively associated with health such as *Veillonella* spp. [14] and the recently characterised *Tannerella* HOT (oral taxon BU063) [15] do not possess sialidases. The apparent importance of sialidases for periodontal pathogens has been investigated in studies of sialidase knockout. *T. forsythia nanH* sialidase mutants displayed decreased attachment to oral epithelial cells compared to their parent strain [16]. Different strains of *P. gingivalis* have also been made deficient in SiaPG [17, 18], although the exact implications for virulence are less clear because the sialidase mutants display defects in capsule formation. Mutant strains do show decreased association with host cells, while the virulence of *ΔsiaPG* mutants in a mouse abscess model is also decreased relative to the parent strain, where subcutaneous injections of wild type *P. gingivalis* (strain W83) resulted in the formation of abscesses and ultimately lethal infection that were not seen in sialidase deficient *P. gingivalis* [17]. Sialidase deficient mutants of *T. denticola* have also been studied, and these display reduced complement evasion and decreased virulence in a mouse abscess model [19].

Given the importance of sialidases for periodontal pathogen-host interactions and subsequent virulence, abrogation of sialidase activity using sialidase inhibitors might exert anti-virulence effects or be detrimental to the lifecycle of these organisms. This is particularly pertinent given recent evidence that levels of sialidase transcript *(T. forsythia nanH* gene) are elevated in periodontal disease [20]. Similarly, sialidase enzyme activity is raised in the gingival crevicular fluid of patients with periodontal disease and this high sialidase activity is an indicator of poor responsiveness to standard treatment [21].

Sialidase inhibitors are undergoing extensive development and some are available as a treatment for influenza, with the sialidase inhibitors oseltamivir and zanamivir licensed for use globally. Sialidase inhibition has been investigated in *T. forsythia*, where the inhibitor oseltamivir was shown to disrupt biofilm formation on host sialoglycan substrates [16]. Considering the above, we set out to further characterise the sialidase of *P. gingivalis*, performing a biochemical characterisation and estabilishing an activity profile while also examining the potential of sialidase inhibitors to modulate pathogenesis of *P. gingivalis* alone and in combination with a range of other periodontal pathogens with the commercially available sialidase inhibitor zanamivir.

Methods

Bacterial strains, human cell lines, and culture conditions *Tannerella forsythia* strains used here were the WT type strain ATCC 43037, supplied by William Wade, Queen Mary University of London, UK, and the sialidase deficient *nanH* mutant (TFΔnanH) [22]. *Porphyromonas gingivalis* strains used here were the WT strains ATCC 33277, 381 (Pg381), and a sialidase deficient mutant of Pg381 (Pg381ΔsiaPG). *Fusobacterium nucleatum* strain NCTC 25586 (subspecies nucleatum) was also used in this study, supplied by William Wade. All strains were cultured at 37 ˚C under anaerobic conditions (10 % CO2, 10 % H2, 80 % N2) in a Don-Whitley mini-macs anaerobic cabinet. *P. gingivalis* and *F. nucleatum* strains were cultured on Fastidious Anaerobe Agar (Lab M, Lancashire, UK) supplemented with 5 % (v/v) oxalated horse blood (Thermo Fisher Scientific, UK), for 2-3 days before harvesting for use in experiments. *T. forsythia* strains were cultured on Fastidious Anaerobe Agar (Lab M, UK) supplemented with 5 % (v/v) oxalated Horse Blood (Thermo Fisher Scientific), 10 μg ml^{-1} N-acetylneuraminic acid (NAM, Sigma Aldrich, UK), and 25 μg ml^{-1} Gentamicin (Sigma-Aldrich) for 3-7 days before harvesting for use in experiments. In addition, TFΔnanH and Pg381ΔSiaPG were intermittently subcultured in the presence of 10 μg ml^{-1} erythromycin to ensure maintenance of the antibiotic resistance cassette marker responsible for sialidase inactivation. Immortalized human oral keratinocytes (OKF6/Tert2) (Dickson et al. 2000) were kindly provided by Dr J. Rheinwald (Harvard Medical School, Cambridge, MA) and were grown in keratinocyte-serum free media supplemented with defined growth supplements (DKSFM, Fisher Scientific, Loughborough, UK). The Oral Squamous Cell Carcinoma (OSCC) cell line H357 (Thomas et al. 2001; Sugiyama et al. 1993)-a generous gift from Professor S. Prime, University of Bristol, UK-was grown in Dulbecco's Modified Eagle Medium (DMEM) supplemented with 10 % (v/v) foetal bovine serum (FBS), 2mM L-glutamine, and 100 units ml^{-1} Penicillin-Streptomycin (Sigma Aldrich). Cells were incubated at 37 ˚C, 5 % CO2 when not undergoing media changes or passaging. Cells were grown to 70–90 % confluence and media was changed every 2–4 days. OBA-9 cells were maintained in keratinocyte basal medium KGM-2 supplemented with epidermal growth factor (EGF), bovine pituitary extract, epinephrine, transferrin, hydrocortisone and insulin, as per the manufacturer's recommendations (Lonza). Cells were used after reaching near confluence.

Cloning, expression, and purification of recombinant proteins NanH and NanS were cloned, expressed, and purified as previously described [23, 24]. A nucleotide sequence encoding SiaPG (PG_0352, based on the genome of strain ATCC 33277) without the secretion signal sequence (supplemental text), was codon optimised for expression in *E. coli*, and synthesized commercially (ThermoFisher). The sequence also contained restriction sites for *NdeI* and *XhoI* at its 5' and 3' ends, enabling it to be ligated into pET vectors. Restriction digest and ligation was performed using NEB buffers, restriction enzymes, and T4 ligase, according to manufacturer's protocols. SiaPG was ligated

into pET21a, and ultimately transformed into chemically competent *E. coli* BL21 (origami B). Expression and purification of recombinant SiaPG was performed as previously described for NanH [24].

Construction of *P. gingivalis siaPG* deletion mutant and genetic complementation.

For generating a sialidase deficient mutant, the *siaPG* gene (PG0352) in *P. gingivalis* 381 strain was inactivated by an allelic replacement strategy. The primers used in the construction and complementation strategy are listed in Table 1. Briefly, a DNA fragment containing PG0352 coding region and flanking sequences was PCR amplified with Primers #1 and #2 using the *P. gingivalis* 381 gDNA. This product was then used as a template to amplify the upstream and downstream regions of PG0352 with primer sets #1 and #3 (for '5 end) and #2 and #5 (for '3 end), respectively. In parallel, the *ermF* gene (797 bp) was amplified from the plasmid pVA2198 with Primers #4 and #6. Primers #3, #4, #5, and #6 contain overlapping sequences for *ermF* and PG0352 to allow generation of a fusion fragment via overlap PCR. Finally, PCR products of PG0352 with flanking regions and *ermF* gene were combined in an overlap PCR reaction using primers #1 and #2. The overlap PCR product was sequenced to confirm the correct fusion of fragments and then transformed into *P. gingivalis* 381 by electroporation as previously described [25]. Transformants were plated on TSB-blood agar plates containing 10 μg ml^{-1} of erythromycin and incubated at 37 °C anaerobically for 10 days. Following incubation, erythromycin-resistant colonies were screened by PCR and Southern blotting. One representative deletion mutant as confirmed by PCR and Southern blotting (data not shown) and showing no sialidase activity was selected and designated as Pg381ΔsiaPG. For complementation of Pg381ΔsiaPG, in trans complementation with the *siaPG* gene on the self-replicating shuttle plasmid pT-COW was employed as we have performed previously [25]. Briefly, the *siaPG* gene fragment amplified by PCR with the primers FWD *BamHI* and REV *SalI* (Table 1) was digested with *BamHI* and *SalI* and ligated into *BamHI* and *SalI* digestd pT-COW plasmid. The resulting plasmid, pT-PG352C was transformation into Pg381ΔsiaPG by tri-parental conjugation involving with Pg381ΔsiaPG, *E. coli* carrying shuttle vector pT-PG352C and *E. coli* carrying helper plasmid pRK231 4,5. The transformants were selected on TSB-blood agar plate containing 100 μg ml^{-1} of gentamicin (Invitrogen), 10 μg ml^{-1} of erythromycin (Sigma) and 1 μg ml^{-1} of tetracycline (Sigma). The completed clones with sialidase expression were saved and one random clone designated Δ*siaPG*$^{+}$ served as a representative.

Inhibition of whole periodontal pathogens and purified sialidases by zanamivir. Zanamivir was provided by GlaxoSmithKline (GSK, Weybridge, UK). Whole *T. forsythia* or *P. gingivalis*, or purified sialidases 2.5 nM NanH or 5 nM rSiaPG were incubated in the presence of 0.1 mM MUNANA, in 50

mM Sodium Phosphate 200 mM NaCl, pH 7.4 (to mimic host physiological conditions), in the presence of different concentrations of zanamivir (0-10 mM). Sialidase inhibition was expressed as the percentage change in fluorescence at a given concentration of inhibitor, relative to fluorescence in the absence of inhibitor. Sialidase inhibition (%) was plotted against log[inhibitor], and the variable slope model applied to obtain the IC50 of zanamivir for SiaPG and NanH in Graphpad Prism 7, using the equation: Y=100/(1+10 (LogIC50-X) × HillSlope). Y = sialidase activity relative to no inhibitor condition (%), X = log[inhibitor], and Hillslope = steepness of the curve.

Biochemistry of SiaPG: Determination of optimum pH, reaction kinetics with MUNANA and sialyllactose, and sialic acid release from mucin in concert with NanS from *T. forsythia.* Whole *P. gingivalis* and purified SiaPG were tested for pH optima in a similar manner to *T. forsythia* and its sialidase [24]. For whole cell assays, bacteria were resuspended from agar plates, washed 3x in phosphate buffer saline, pH 7.4 (PBS, Sigma Aldrich) and centrifugation at 10000 *g* for 2 minutes, and resuspended to an OD600 of 0.05 in appropriate reaction buffers (20 mM sodium citrate–citric acid (pH 3.0–6.4), sodium phosphate mono-basic/dibasic (pH 6.8–8.8) or sodium carbonate–sodium bicarbonate (pH 9.2–10.5)). For pH optimum derivation for purified SiaPG, enzyme was used at 2.5 nM. In both cases, cells or enzyme were incubated with 100 µM Mu-NANA and quenched with addition of 100 mM sodium carbonate buffer, pH 10.5, at a volume ratio of 1 : 1.5 (reaction: sodium carbonate), and sialidase activity quantified by measuring 4-MU fluorescence (λex = 350 nm; λem = 450 nm). For whole *P. gingivalis* assays were performed over 1-3 hours at 37 °C, incubation with SiaPG was performed over 1-3 minutes at room temperature (~20 °C).

For derivation of Michaelis-Menten kinetics for SiaPG, 2.5 nM enzyme was incubated with varying concentrations of MU-NANA and again quenched. A standard curve of the fluorescence signal of 4-MU at defined concentrations was also obtained, enabling sialidase activity to be expressed as 4-MU released µmol min^{-1} mg^{-1} SiaPG. Similar conditions were used for derivation of kinetic parameters with 3/6-siallyl-lactose, except no quenching was required and the levels of released sialic acid using a modified Thiobarbituric acid (TBA) assay. In this case reactions were stopped at time points over 1-5 minutes by commencement of the TBA assay: Fifty microlitres of these reactions were added to 25 µl of 25 mM sodium periodate (Sigma–Aldrich) in 60 mM H_2SO_4 (Thermo Fisher) and incubated for 30 min at 37 °C. This oxidation step was stopped by the addition of 20 µl of 2% (w/v) sodium meta-arsenite (Sigma–Aldrich) in 500 mM HCl. Forty-seven microlitres of this reaction were added to 100 µl of 100 mM TBA, pH 9.0, and incubated at 95 °C for 7.5 min, resulting in the thiol-labelling of free sialic acid. Upon centrifugation at 1500 G for 5 min, the pink chromophore in the clarified supernatant was spectrophotometrically quantified at A_{549}. A standard curve of known sialic acid

(Neu5Ac, Carbosynth) concentrations was used to calculate sialic acid release in µmolmin^{-1}mg^{-1} SiaPG. Finally, release of Neu5Ac from mucin was assessed using BSM and the TBA assay. PBS + 6 µM BSM was incubated with combinations of 100 nM rSiaPG, 0.5 mM zanamivir, and/or the sialate-O-acetylesterase NanS from *T. forsythia* (100 nM), and incubated for 30 minutes at 37 °C, before the reaction was stopped and the TBA assay commenced as described above.

Analysis of Procainamide labelled glycans. SLeX and FA2G2S2 (A2F) glycans (Ludger Ltd.) underwent procainamide labelling (see below), as were glycans released from recombinant human EPO as previously described [23]. Briefly, human EPO was expressed in Chinese hamster ovary (CHO) cells (a gift from Antonio Vallin, Center for Molecular Immunology, La Habana, Cuba) and released using peptide N-glycosidase F (PNGase F, E-PNG01; Ludger Ltd). EPO (in 17.5 µl) was denatured at 100 °C for 5 mins with the addition of 6.25 µl 2 % (w/v) SDS, and 1 M 2-mercaptoethanol, then incubated at 37 °C for 16 h with 1 µl PNGase F and 1.25 µl 15 % (w/v) Triton X-100. Released N-glycans were fluorescently labelled with 2-aminobenzamide (2-AB) as described previously [26] using a LT-KPROC-96 kit (Ludger Ltd.). The released glycans were incubated with labelling reagents for 3 h at 65 °C. The 2-AB- labelled glycans were cleaned up using LudgerClean S Cartridges (Ludger Ltd), then incubated with 1 µl of 1 mg ml^{-1} SiaPG in a final volume of 10 µl (50 mM sodium acetate buffer, pH 5.5) for 16 h at 37 °C. Glycans were cleaned-up and SiaPG removed using a LC-PROC-96 kit (Ludger Ltd.) Procainamide labelled glycans (Ludger) were analysed by UHPLC-MS/MS. Here, 25 µl of each sample was injected into a Waters ACQUITY UPLC Glycan BEH Amide column (2.1 x 150 mm, 1.7 µm particle size, 130 Å pore size) at 40°C on a Dionex Ultimate 3000 UHPLC instrument with a fluorescence detector (λex = 310 nm, λem = 370 nm) attached to a Bruker Amazon Speed ETD. Mobile phase A was a 50 mM ammonium formate solution (pH 4.4) and mobile phase B was neat acetonitrile. Analyte separation was accomplished by a gradient running from 76-51% mobile phase B over 70 minutes at a flow rate of 0.4 ml min^{-1}. The Amazon Speed was operated in the positive sensitivity mode using following settings: source temperature, 180 C; gas flow, 4 L min^{-1}; capillary voltage, 4500 V; ICC target, 200,000; maximum accumulation time, 50.00 ms; rolling average, 2; number of precursor ions selected, 3; scan mode, enhanced resolution; mass range scanned, 400 to 1700. Data was analysed using Bruker Compass Data Analysis software v4.1 and glycan diagrams made using GlycoWorkbench v2.0. Glycan compositions were elucidated based on MS2 fragmentation.

Lectin staining for cell surface sialic acid- immunofluorescence microscopy. H357 cells were seeded at a density of 1.5x10^5 cells ml^{-1} into the wells of a 24-well tissue culture plate which contained sterile glass coverslips (BDH). These were incubated at 37 °C, 5 % CO_2 for 18 hours. Treatment with

SiaPG and NanH was performed by washing 2 x with PBS, then incubated with 200 nM of each sialidase for 30 minutes at 37 °C. Cells then underwent sialic acid staining with lectins from *Sambucus nigra* (FITC conjugated SNA, Vector Labs, specific for α2-6 Neu5Ac linkages), *Maackia amuriensis* (Biotinylated MAA, Vector Labs, specific for α2-3 Neu5Ac linkages). After treatment, cells were washed twice with 500 µl PBS followed by application of lectins: 4 µg ml^{-1} SNA or 8 µg ml^{-1} MAA, for 30 minutes at 37 °C, 5 % CO2. Cells were washed twice with 500 µl PBS, and conditions containing MAA underwent a second incubation with 2 µg ml^{-1} Texas Red-Streptavidin, for 30 minutes at 37 °C. Stained cells were washed three times with 500 µl PBS and fixed with 500 µl 2 % (w/v) paraformaldehyde for 15 minutes at 37 °C. Coverslips with fixed cells were removed from wells and mounted onto glass slides with ProLong Gold Antifade mount (containing DAPI, ThermoFisher Scientific). Mounted cells were incubated for at least 18 hours and visualised within one week. Imaging was performed with an Axiovert 200M fluorescence microscope (Zeiss) and associated Axiovert software (Zeiss). Images were processed using Fiji-imageJ, Software [27]. Fluorescence background subtraction was performed for all images using the same parameters for each fluorescence colour channel in a given experiment.

Biofilm assays. *P. gingivalis* was cultured in the wells of a 96-well tissue culture plate (poly-lysine coated, Greiner): Bacteria from an agar plate were resuspended to an OD600 of 0.05 in Tryptic Soy Broth (TSB; Sigma-Aldrich) supplemented with 2 % (w/v) yeast extract, 1 µg ml^{-1} vitamin K, 5 µg ml^{-1} hemin, 50 µg ml^{-1} gentamicin, and either 6 mM Neu5Ac or no additional supplements. In conditions testing host glycoproteins, 100 µl of 6 µM BSM, 100 % (v/v) pooled human saliva, or fetal bovine serum (FBS) was added to plate wells and left to coat the wells by incubation at 4 °C overnight, removed, and wells washed with PBS once. In conditions testing the effect of sialidase inhibition, 10 mM zanamivir was included. All media was equilibrated overnight in culture conditions, namely, 37 ˚C under anaerobic atmosphere (10 % CO_2, 10 % H_2, 80 % N_2). Biofilms were cultured for 5 days. To quantify planktonic or total growth, all conditions underwent OD_{600} measurement using a Tecan Infinite M200 plate reader. Quantification was carried out by either crystal violet staining or manual counting of organisms. Crystal violet solution (0.1 % w/v) was added to each well and incubated at room temperature for 30 minutes. After incubation, crystal violet was removed and wells were gently washed 3-4 times with PBS before visualisation using light microscopy or extraction with 80: 20 ethanol: acetone. For manual counting, biofilms were gently washed twice using PBS to remove planktonic cells, and vigorously resuspended in PBS and serial diluted where appropriate. Bacteria were enumerated by counting using a Helber chamber (Hawksley) under phase contrast microscopy, 400 x magnification.

Antibiotic protection assays H357 or OKF6 cells were seeded into the wells of a 24-well tissue culture plate at a density of 1.2 x 10^5-2 x 10^5 cells and incubated for 24-48h. Media was removed, the cells in one well were detached by trypsinisation and counted by haemocytometry, to determine the number of cells per well. Remaining cells were incubated for 1 hour in media supplemented with 2 % (w/v) bovine serum albumin (BSA), then washed twice with PBS. Bacteria were quantified using a Helber chamber (Hawksley) under phase contrast microscopy, 400 x magnification. Bacterial suspensions were diluted in culture media (with no FBS or antibiotics) to a ratio of 1:100 host cells: bacteria, and for inhibitor testing conditions 10 mM zanamivir was included. These suspensions were incubated with the host cells at 37 °C, 5 % CO2 for 1.5 hours, or in empty wells containing no host cells-constituting a bacterial "viability" control. After incubation, the wells were washed twice with PBS, and either harvested (see below)-forming the "total association" condition, or media with 200 µg ml^{-1} metronidazole was added, then incubated at 37 °C, 5 % CO_2 for 1 hour, forming the "invasion" conditions. To harvest bacteria, wells were washed three times with PBS, lysed with deionised water and scraped with a pipette tip for one minute. Sufficient lysis was checked by microscopy (this method reliably resulted in >99 % lysis). Harvested bacterial suspensions underwent serial dilutions and were plated onto agar by Miles-Misra methodology. After incubation and colony counting, the number of bacteria associated with host cells was determined and expressed as a percentage of viable bacteria that were associated with and had invaded the OKF6 cells. By subtracting invaded organisms from associated, the number of "attached" bacteria was obtained.

Assessment of zanamivir cytotoxicity Quantifying metabolism as an indicator of cell viability was performed using 3-(4,5-Dimethylthiazol-2-yl)-2,5-Diphenyltetrazolium Bromide (MTT). Twenty five thousand OKF6 cells in DKSFM were seeded into the wells of a 96 well tissue culture plate (Greiner), and incubated for 24 hours at 37 °C, 5 % CO_2. Cells were then washed twice with PBS, and media supplemented with 1 mg ml^{-1} MTT, and 0, 2.5, 5, 7.5, or 10 mM zanamivir was added. Cells were incubated for 2.5 hours at 37 °C, 5 % CO_2. MTT-supplemented media was removed, and cells were washed twice using PBS. Formazan crystals were solubilised using isopropanol + 0.125 % (v/v) HCl, and quantified by measuring absorbance at 540 nm, reference at 630 nm using a Tecan Infinite M200 plate reader. A commercially available lactate dehydrogenase (LDH) assay, Cytotox 96 (Promega) was also used to assess cell membrane permeability as a measure of viability, according to manufacturers' instructions, with cells seeded as described for MTT assays.

Results

SiaPG is a highly active, broad specificity sialidase, and desialylates host glycans. The coding sequence of SiaPG without secretion signal sequence was synthesized as a codon optimised fragment and cloned into a pET21a plasmid. Expression was performed in *E. coli* BL21 (origami B), and purified via Nickel affinity chromatography to high homogeneity (supplemental figure S1). The commonly used fluorogenic 4-methylumbeliferyl-N-acetyl neuraminic acid (MUNANA) substrate was used to assess sialidase activity with liberated 4-methylumbelliferone (4-MU) measured with fluorescence change per minute used to quantify sialidase activity (Figure 1 A). We observed that SiaPG has optimal activity under acidic conditions, with highest activity observed at a pH of 5.2-5.6. However, it retained 40-50 % activity between pH 4.4 and 7.2, and ~20-30 % retained even at pH 4 and 8. Whole bacterial sialidase activity of *P. gingivalis* was also assessed, finding that ≥~70 % maximal activity was retained in the pH range 4.8-8.0, with the highest activity observed at pH 6.8, (Figure 1 B). The stronger activity of whole *P. gingivalis* sialidase in a wider pH range compared to the sialidase protein may be due to a buffering or stabilising effect of cell membranes or other components and is relevant given that subgingival GCF pH is in the neutral range.

We also performed kinetics experiments to enable comparison of SiaPG to other sialidases. Given the pH variations in the pathogens' ecological niche, i.e. the conditions the sialidases would encounter in the host, we evaluated sialidase activity at SiaPG-optimum (pH 5.6) as well as physiological pH (7.4) that would be present in the mouth, and in the presence and absence of additional salt (figure 2). SiaPG had the greatest catalytic efficiency (k_{cat}/K_M) at pH 5.6 in the presence of salt (161.0 μM min^{-1} with 200 mM NaCl, 124.7 μM min^{-}without NaCl). At pH 7.4, salt had a similar impact on catalytic efficiency of SiaPG (49.9 μM $min^{-}$with NaCl, 36.4 μM min^{-}without NaCl). These values are broadly in line with those previously reported for the NanH sialidase of *T. forsythia* [24], though salt had the opposite effect on NanH catalytic efficiency.

In addition to MUNANA, we assessed the ability of SiaPG to cleave 2-3' and 2-6' linked sialic acid, initially with the trisaccharide substrate sialyllactose (3- and 6- sialyllactose), using a TBA assay as previously described for NanH. SiaPG was capable of cleaving both linkage types (Figure 3), and although it had a much higher affinity (lower K_M) for the 2,6 linkage than 2,3, its reaction velocity with the 2,3 version means that it has a ~50 % higher catalytic efficiencies (K_{cat}/K_M) for the 3-sialyllactose linked sugars.

Desialylation of more complex and physiologically relevant glycans by SiaPG was also assessed using HPLC and mass spectrometry. SLeX is an oligosaccharide containing α2-3 linked sialic acid, and is present in numerous host niches-on the plasma membrane of various cell types and at the termini of secreted glycans. SLeX may also play a role in *P. gingivalis* pathogenesis [28]. We

exposed soluble SLeX to SiaPG, subjected the reaction to HPLC, and found that SLeX was efficiently desialylated by SiaPG (Figure 4A). Cleavage of α2-6 linked sialic acid by SiaPG was tested using the host-relevant FA2G2S2 (also known as A2F) glycan, a two-branched polysaccharide chain where both branches terminate with a sialic acid, which is present on a number of secreted glycoproteins including IgG. SiaPG was again capable of desialylating FA2G2S2 (Figure 4B). Notably, other peaks were observed in the chromatogram for FA2G2S2, which are likely to correspond to differently sialylated versions of the FA2G2S2 glycan, and these also appeared to be desialylated - notably the mammalian NeuGc versions. It would be interesting to test the activity of SiaPG against such NeuGc linked glycoconjugates, which the human host does not synthesize but obtains from dietary sources.

Finally, we wanted to test desialylation of glycans derived from a complex sialoglycoprotein by SiaPG. To this end, we chose the host glycoprotein erythropoietin (EPO) due to its possession of multiple bi-, tri- and tetra- branched glycans, the presence of α2-3 and α2-6 sialic acid linkages, and because some of its NeuAc is mono or di-O-acetylated (Neu5,9Ac, and perhaps tri-acetylated Neu5,8,9Ac). EPO was digested with SiaPG, N-glycans were procainamide labelled, and these underwent UHPLC-MS/MS (Figure 5). As expected, the UHPLC chromatogram of undigested EPO showed the presence of multiple peaks corresponding to various EPO glycans, further details and structures of these are shown in supplemental table 1. Following digestion with SiaPG, we observed a marked change in the chromatogram. The remaining peaks were investigated by MS/MS, providing evidence that SiaPG was able to cleave the sialic acid from a wide-range of glycan structures. However, this analysis also revealed the inability of SiaPG to cleave diacetylated (or triacetylated) sialic acids (Figure 5, lower 2 panels). These analyses showed that extracted ion chromatogram (EIC) corresponding to the MS2 ion for Neu5Ac trisaccharide (GlcNAc-Gal-Neu5Ac, *m/z* = ~657.25) was not detected above background levels, while EIC corresponding to di- and tri- acetylated sialic acid trisaccharides (GlcNAc-Gal-Neu5,9Ac and GlcNAc-Gal-Neu5,8,9Ac, *m/z* = ~699.25 and ~741.26) were detected in high abundance (high peak intensity)- i.e. had been left uncleaved by SiaPG; a result expected given our previous studies on NanH [23].

SiaPG releases Neu5Ac from mucins, an activity enhanced by the sialate-O-acetylesterase NanS from *T. forsythia*. To explore activity of SiaPG further we next tested its activity with a glycoprotein substrate relevant in the oral cavity- salivary mucin. Notably the commonly used Bovine Submaxillary mucin (BSM) used in these experiments contains many terminal sialic acids that have the second O-acetyl group, i.e. contain Neu5,9Ac [29]. Our previous data on NanH [23] and SiaPG (this study) indicate terminal Neu5,9Ac is resistant to cleavage by periodontal sialidases. To counter this, some bacteria express sialate-O-acetylesterases, such as NanS from *T. forsythia*, which remove

the second acetylation (forming Neu5Ac), and rendering the sialic acid susceptible to sialidase cleavage. Indeed, we previously demonstrated that *T. forsythia* NanS enhances NanH sialidase activity on Neu5,9Ac terminal sugars and may act to aid sialidases from other species in harversting sialic acid [23]. To test the hypothesis that *T. forsythia* may act to enhance SiaPG activity we performed sialic acid release assays on BSM. The data showed that NanS enhanced sialic acid release by SiaPG from BSM by ~2.5 -fold (from 302 to 746 pmol/min) (Figure. 7).

Zanamivir more efficiently inhibits sialidase activity of SiaPG and whole *P. gingivalis* than sialidase activity of *T. forsythia* NanH and whole *T. forsythia*. As outlined, one aim of this study was to assess the ability of a safe and FDA-approved drug in its ability to potentially reduce virulence of the keystone periodontal pathogen, *P. gingivalis*. Therefore we assessed the impact of zanamivir on the activity of whole *P. gingivalis* and another periodontal pathogen, *T. forsythia*, as well as their purified sialidases using the MUNANA assay as described above. Both pathogens and purified sialidases displayed decreased sialidase activity as zanamivir concentration was increased (Figure 6 A). The decrease in activity was far more drastic for *P. gingivalis*, with a decrease in activity of ~70 % in the presence of 10 mM zanamivir, compared to *T. forsythia* which only showed a decrease of ~25 % (Figure 6 B). This apparent difference in efficacy for the two sialidases was confirmed by establishing the IC50 of zanamivir for purified SiaPG and NanH (Figure 6 B), where zanamivir displayed a greater inhibitory effect on SiaPG (369 µM) than NanH (6130 µM). These data were further enhanced when we observed that zanamivir also inhibited sialidase activity in the context of removal of sialic acid from mucin (Figure 7). There was no effect on NanS sialate-*O*-acetylesterase activity alone (data not shown).

***P. gingivalis* biofilms on host sialoglycans are sialidase-dependent and disrupted by zanamivir.** *P. gingivalis* was cultured in microtitre plates, where well surfaces were coated with mucin (BSM), saliva (pooled human saliva), or serum (FCS) in the presence or absence of 10 mM zanamivir. Total growth (Figure 8 A) of *P. gingivalis* in the mucin-coated condition was significantly reduced in the presence of zanamivir, from OD600 0.21 to 0.11 ($p = <0.001$) i.e. zanamivir reduced total growth of *P. gingivalis* in mucin-coated conditions by approximately half. In the presence of the other glycoprotein-coated conditions (saliva and serum) there was a trend towards small reductions in total growth in the presence of zanamivir but these did not reach statistical significance. Biofilm formation (normalised to total growth-optical density) of *P. gingivalis* (Figure 8 B) was also reduced when grown on mucin coated surfaces (30-40 % reduction, $p = <0.01$), indicating that biofilm formation on these surfaces was inhibited by zanamivir. Notably we also saw a consistent small

reduction on serum, but total growth (OD600) standardised to biofilm formation (bacteria ml^{-1}) of cultures grown on human saliva-coated surfaces was too variable to make conclusions.

In support of our evidence that sialidase is important when *P. gingivalis* grows on mucin coated surfaces (as would often be the case *in vivo*), we also tested the effect of sialidase activity in this regard in a related *P. gingivalis* strain – 381 (Pg381). For this purpose, a *siaPG* deletion mutant of *P. gingivalis* 381 and its complememted strain were constructed (Pg381ΔsiaPG and ΔsiaPG+). Pg381ΔsiaPG showed no sialidase activity as judged from lack of fluorescence on incubation with MUNANA, while the silaidase activity was restored in the comlemented strain $\Delta siaPG^{+}$ (supplemental figure S2). In biofilm assays, we observed a 2-fold reduction in biofilm growth in Pg381ΔsiaPG (relative to the WT) on mucin coated surfaces, with this phenotype complemented by provision of the SiaPG gene in the mutant (ΔsiaPG+, figure. 9). These data expand our view of the role of sialidase to a range of *P. gingivalis* strains and suggest it may be true across this species.

SiaPG releases 3- and 6- linked sialic acid from oral epithelial cells and is inhibited by zanamivir. Studies of mutant strains and purified enzymes have shown that the well-studied *T. forsythia* NanH can desialate oral epithelial cells [22, 24], while SiaPG mutant strains have been used to highlight *P. gingivalis* sialidase-mediated release of sialic acid from erythrocytes [18]. In order to test the effect of SiaPG on physiologically relevant oral epithelial cells, we stained the OSCC line H357 with the lectins SNA and MAA enabling fluorescent imaging of cell surface α2-3 and α2-6- linked sialic acid. Exposure of epithelial cells to SiaPG (and *T. forsythia* NanH) was successful in desialylating cell surfaces (this had been shown previously for NanH [22]), while 10 mM zanamivir inhibited desialylation in the case of SiaPG, but not NanH (figure 10, supplemental figure S3).

Zanamivir inhibits periodontal pathogen-host cell association during monospecies infection. One established aspect of *P. gingivalis* virulence is its ability to invade and reside within oral epithelial cells. To this end we performed antibiotic protection assays to establish whether zanamivir had any potential effect on host cell interaction and invasion. However, the effects of zanamivir on bacterial and human cell viability had to be established. To this end, oral epithelial cells were subjected to 10 mM zanamivir under antibiotic protection assay conditions, illustrating no effect of zanamivir on either membrane integrity (assayed by LDH) or cellular activity/ viability (via MTT assay) (supplemental figure S4). Similarly, we incubated *P. gingivalis*, *T. forsythia* and *F. nucleatum* with zanamivir under antibiotic protection assay conditions (2.5 hours in tissue culture medium), before obtaining cfu counts, and revealed no detrimental effect of zanamivir on viability of any of these species (supplemental figure S5).

Next we performed antibiotic protection assays on two oral epithelial cell lines, namely the OSCC cell line H357- a frequently used model for oral epithelium-bacteria interactions in our laboratory [30, 31] and normal immortalised oral epithelial cell line OKF6 [32, 33]. In addition to *P. gingivalis* we also tested the effect of zanamivir on two other key periodontal pathogens- namely *T. forsythia* and *F. nucleatum* subsp. *nucleatum*. For all three pathogens, in both cell lines, zanamivir significantly reduced one or more aspects of host-bacteria association in both cell lines (figure 11). For *T. forsythia*, attachment, invasion, and total association (the sum of attached and invaded bacteria) were all significantly reduced in both cell lines; from 3.2 to 1.0 %, 2.5 to 0.3 %, and 5.8 to 1.4 % in OKF6 cells, and 4.6 to 1.2 %, 3.4 to 1.6 %, and 8.0 to 2.8 % in H357 cells (figure 11 A). For *P. gingivalis*, attachment, invasion, and total association were significantly reduced in OKF6 cells; from 0.9 to 0.1 %, 0.7 to 0.1 %, and 1.7 to 0.2 %, however in the H357 cell line, only invasion was significantly reduced, from 4.5 to 1.8 % (figure 11 B). Finally, for *F. nucleatum*, invasion and total association were significantly reduced in OKF6 cells; from 4.6 % to 1.3 %, and 5.6 to 2.6 %. For H357 cells attachment and total association were significantly reduced 21.8 % to 7.2 %, and 36.6 % to 18.2 % (figure 11 C).

To support the notion that sialidase activity is important for bacteria-host cell association, rather than disruption of other processes by the presence of zanamivir, the human gingival cell line OBA-9 was exposed to *P. gingivalis* 381 (Pg381) and a *siaPG* deficient mutant (Pg381Δ*siaPG*). Exposure to the latter strain was performed without or with exogenous SiaPG . Pg381Δ*siaPG* displayed significantly decreased association with host cells relative to the parent Pg381, which was restored by the presence of exogenous SiaPG in a concentration dependent manner (supplemental figure S6): While 100 μg ml^{-1} exogenous recombinant SiaPG resulted in partial restoration of host-bacteria association of Pg381Δ*siaPG* (WT; 0.50 %, Pg381Δ*siaPG* ; 0.15 %, Pg381Δ*siaPG*+100 μg SiaPG ; 0.26), 200 μg/ml SiaPG resulted in complete restoration of host-bacterial association Pg381 (0.58 %).

Zanamivir inhibits attachment and invasion of oral epithelial cells during infection with multiple periodontal pathogens. To at least partially mimic the *in vivo* situation, where none of these species exist in isolation, we performed antibiotic protection assays where multiple periodontal pathogens were used to infect cells. This is particularly relevant during host cell association, since periodontal pathogens have been shown to act in synergy during attachment and invasion [34–36]. MOI was maintained at 1:100 host cells: bacteria, so for infections using two species, the ratio was 1:50:50 (host cells: species 1: species 2), and for infections with all three species, the ratio was 1:33:33:33 (host cells: species 1: species 2: species 3). *T. forsythia, P. gingivalis, and F. nucleatum* were used in a variety of combinations to infect epithelial cells. In addition to quantifying the numbers of all

bacteria-not distinguishing between species during an assay-the levels of each individual species in a given assay could be enumerated by colony counting on agar plates, since the colony morphologies of *T. forsythia*, *F. nucleatum*, and *P. gingivalis* are distinct from each other (supplemental figure S7). All possible combinations were tested in this way. For ease of discussion, only the total number of bacteria in each combination are described here, with complete results for each individual species provided in supplemental figures S8-S11. For *T. forsythia* and *F. nucleatum* co-infection, zanamivir significantly reduced both invasion and total association of bacteria with host cells, from 7.4 to 1.8 %, and 19.6 to 7.6 % ($p<0.01$ and $p<0.05$), respectively (Figure 12 A). For *T. forsythia* and *P. gingivalis* co-infection, the variation between experiments meant that none of the reductions were statistically significant (where $p <0.05$, Figure 12 B), i.e. attachment was reduced from 12.1 to 0.8 % ($p=0.076$), invasion from 2.8 to 1.4 % ($p=0.25$), and total association from 14.4 to 2.5 % ($p=0.062$). For *F. nucleatum* and *P. gingivalis*, zanamivir significantly reduced attachment, invasion, and total association of bacteria with host cells, from 1.9 to 0.8 % ($p=<0.05$), 4.0 to 1.56 % ($p=<0.05$), and 5.9 to 2.4 % ($p=<0.01$), respectively (figure 12 C). Finally, all three species (i.e. *T. forsythia, F. nucleatum* and *P. gingivalis*) were infected into the cells as a three-species community. Here, strikingly, zanamivir significantly reduced attachment, invasion, and total association of bacteria with host cells, from 17.7 to 7.7 % ($p = <0.001$), 9.6 to 7.15 % (, $p = <0.05$), and 26.14 to 14.6 % ($p = <0.001$), respectively (figure 12 D); indicating this approach might have impact on cellular interaction *in vivo*.

Discussion

In this study we characterised the activity of the sialidase (SiaPG) from *P. gingivalis* on a number of glycan and proteinaceous substrates, including relevant host sialoglycans SleX, FA2G2S2 and EPO, and establishing activity across a range of pH values. During these studies, it became apparent that SiaPG could cleave both α2-3 and α2-6 linked Neu5Ac, but not diacetylated Neu5,9Ac. These data also agreed with low sialic acid release from the heavily diacetylated BSM protein, and this activity being enhanced by coincubation with an enzyme capable of removing O-acetyl groups on sialic acid residues - namely the NanS sialate-*O*-acetylesterase from the fellow oral bacterium *T. forsythia* [23]. We hypothesise that *in vivo* NanS enhances the ability of *P. gingivalis* to cleave sialic acid from glycoproteins - although given the fact that *P. gingivalis* does not produce its own esterase or utilise sialic acid for nutrition we can only postulate that somehow removal of sialic acid opens up sites for adhesion to oral surfaces, or might modulate immune responses mediated by Siglecs (sialic acid-binding immunoglobulin-like lectins) or allow *P. gingivalis* to access underlying sugars or the protein component of the glycoproteins themselves, and may explain synergies between these organisms observed by others [37–39].

We tested the ability of zanamivir to inhibit SiaPG and the previously characterised NanH sialidase from another red complex pathogen, *T. forsythia*. While the inhibition (IC50) of SiaPG activity on MUNANA was determined to be within the micromolar range (~350 μM), this was not the case for *T. forsythia*, which required >6 mM zanamivir to reduce its activity by half. A similar trend was also seen for whole bacteria. The relatively low efficacy of zanamivir for some bacterial sialidases is observed in other studies where sialidases from the pathogens *S. pneumoniae* and *Gardnerella vaginalis* are apparently only inhibited to limited extents [40, 41]. Nevertheless, here we showed that *P. gingivalis* sialidase was effectively inhibited by zanamivir. At present we have no mechanistic explanation for the variation between the two sialidases, but postulate it may result from structural differences, despite both possessing typical catalytic GH33 domains with predicted 6-blade propeller structures the sialidases only share 23 % amino acid sequence identity.

Given this, and the ability of SiaPG to cleave sialic acid from complex glycans (FA2G2S2, EPO), we assessed the ability of SiaPG to remove sialoglycans from oral epithelial cells, illustrating removal in both cases and highlighting the broad glycan specificity of this enzyme and the ability of zanamivir to affect this process. As shown previously, NanH was also capable of desialylating oral epithelial cells [22].

Considering the ability of zanamivir to inhibit *P. gingivalis* sialidase activity, *in vitro* virulence models were carried out. It has been shown previously that NanH is key during biofilm formation in *T. forsythia*, and that sialidase inhibitors are also detrimental to *T. forsythia* biofilms [42]. We observed that sialidase inhibitors decreased *P. gingivalis* biofilm formation on host glycoprotein sources, significantly on saliva and mucin. In addition, biofilm formation of sialidase deficient *P. gingivalis* on mucin was reduced compared to its parent, and restored upon complementation. Biofilms of sialidase deficient *P. gingivalis* are also reduced on plastic surfaces [17]. There are various mechanisms by which sialidase activity may contribute to *P. gingivalis* biofilm formation. Possibilities include decreased proteolysis and subsequent nutrient deficiency or an inability to attach to cleaved proteins, since sialylation may protect against proteolytic activity [43]. Interference with the *P. gingivalis* capsule is also possible, sialidase expression appears to be important for *P. gingivalis* capsular synthesis, mutants deficient in SiaPG show reduced capsule formation [17, 18], and yet loss of the capsule has been shown to enhance biofilm formation [44], thus, we might expect zanamivir (or sialidase knockout) to enhance biofilm formation, but here we observed the opposite, possibly because non-capsulated (fimbriated) strains were tested. In any case, we cannot rule out the possibility that sialidase inhibition may interfere with capsular structure or interactions in the case of *P. gingivalis* strains which are encapsulated. Finally, maturation and processing of gingipains-

proteases central to *P. gingivalis* virulence and asacharolytic nutrition-is also altered in sialidase deficient mutants [18]. Zanamivir may impact biofilm formation through any, or all, of these mechanisms. It would be particularly interesting to assess the impact of zanamivir on mixed-species biofilms, and in addition to direct impacts on sialic acid-mediated interactions and any indirect effects that may result from sialidase inhibition. For example, it has been previously shown that lysine gingipains (Kgp) of *P. gingivalis* mediate *T. forsythia* levels in mixed species biofilms [45], and . given that sialylation may influence protease access to protein backbones, inhibition of *P. gingivalis* sialidase may also impact the activity of Kgp, subsequently reproducing the detrimental effect of Kgp deficiency on *T. forsythia* abundance. Similarly, it has been noted that *T. forsythia* surface S-layer glycans play a potential role in localisation with *P. gingivalis* within polymicrobial biofilms [46]. These glycans contain terminal nonulosonic analogues of sialic acid (pseudaminic and legianaminic acids) and it is possible that Zanamivir may influence these interactions as a glycan mimic.

Given that periodontal pathogen sialidases have been shown to be important during host cell association [17, 18, 22, 42] and zanamivir inhibited host cell surface desialylation by SiaPG, but not *T. forsythia* NanH, it might be expected that zanamivir would decrease attachment and invasion of host cells by *P. gingivalis* but not *T. forsythia*. Surprisingly, host cell association was greatly inhibited in the case of both organisms, and in the sialidase negative *F. nucleatum* [13]. Of note here is that while our data re-emphasize the role of sialidase in the equivalent *P. gingivalis* capsulated W83 strain [18], indicating that this phenotype is widespread in *P. gingivalis,* it would be of interest to establish whether zanamavir has the same effect on capsulated strains. It is also possible that other periodontal pathogen virulence factors are inhibited by zanamivir. For example, the adhesin FadA is highly conserved among oral fusobacteria, and considered important for association with oral epithelial cells [47] and has been shown to bind cell surface E-selectin, whose native ligand is a sialoglycan (sialyl lewis A/X), so perhaps a sialic acid analogue might interfere with FadA-host cell surface interactions.

Although the monospecies antibiotic protection assays hinted at the usefulness of zanamivir as an anti-virulence therapeutic, periodontitis is mediated by a dysbiotic polymicrobial community. Therefore, we performed mixed species antibiotic protection assays with combinations of all three of the periodontal pathogens from the monospecies antibiotic protection assays. Importantly, zanamivir influenced invasion in the triple-species infection model with *F. nucleatum*, *P. gingivalis*, and *T. forsythia*. Despite evidence of synergy in invasive capability reported in the literature [34, 36, 48] we were surprised zanamivir effected all species in these assays, given that *F. nucleatum* has no sialidase and *T. forsythia* sialidase is only weakly inhibited by zanamivir. One explanation might be

that only a modest reduction in sialidase activity can reduce invasion for *T. forsythia*. However, zanamivir acts on host sialidases, in particular Neu1 and Neu3, which contribute to the immune response to bacteria via TLRs, where host sialidases are mobilised to the plasma membrane where they activate TLRs 2-, 3- and 4- [49-51], and zanamivir (and other sialidase inhibitors) has been shown to inhibit TLR activation by LPS [52]. Inhibition of host cell sialidases by zanamivir may therefore affect the cell surface charge and glycosylation state of receptors involved in bacterial adhesion and invasion. Indeed our data may suggest that there are host and bacterial sialidase dependent events that not only warrant further study but make a strong case for the potential of these inhibitors to affect periodontal disease pathogenesis, since they may have dual action on host and bacterial processes.

Conclusion

In summary, we further characterised the sialidase of *P. gingivalis*, and provided evidence advocating for the development of sialidase inhibitors as therapeutics for periodontitis-and other diseases-where bacterial sialidases play key roles in virulence. Zanamivir was capable of inhibiting sialidase activity and virulence mechanisms of *P. gingivalis*, most prominently host cell association. However, our study raises several questions and directions for further work, most notably that host as well as bacterial sialidase may influence interactions more than currently understood. Ultimately, sialidase inhibition represents a potential novel therapy for periodontal and other diseases, and merits further investigation. Finally, zanamivir is a safe and efficacious drug for treatment of influenza, but clearly only inhibits bacterial sialidases relatively weakly (µM –mM range). However, its effectiveness in this study suggests that the development of more potent and selective inhibitors of bacterial sialidase should be a focus in upcoming years as they may hold potential as a safe and efficacious treatment in periodontal and other diseases.

Author statements

Funding: AF and MS were funded by a BBSRC iCASE studentships (BB/K501098/1, BB/M01570X/1), while CP was funded by a grant from the Dunhill Medical Trust to GS (DMT-R185/0211). We acknowledge the funding form NIH grant DE14749 to AS and William M. Feagans Endowed Chair Research Fund, University at Buffalo School of Dental Medicine to KH.

Conflict of **Interest**: We declare no conflicts of interest, besides the provision of zanamivir by GlaxoSmithKline (GSK), Stevenage, UK, and AF was sponsored by a BBSRC iCASE studentship (BB/K501098/1) in partnership with GSK.

Author contributions: AF, GS, JP and DB devised the concept of the work. AF, MS, PU, DS, KH and CP performed aspects of lab analysis. AF, GS and AS drafted and wrote the manuscript. All authors contributed to editing of the paper.

Bibliography

1. **Hajishengallis G, Darveau RP, Curtis MA**. The keystone-pathogen hypothesis. *Nat Rev Microbiol* 2012;10:717–725.

2. **Meuric V, Le Gall-David S, Boyer E, Acuña-Amador L, Martin B, *et al.*** Signature of microbial dysbiosis in periodontitis. *Appl Environ Microbiol* 2017;83:1–13.

3. **Socransky SS, Haffajee a D, Cugini M a, Smith C, Kent RL**. Microbial complexes in subgingival plaque. *J Clin Periodontol* 1998;25:134–44.

4. **Ximénez-Fyvie L a, Haffajee a D, Socransky SS**. Comparison of the microbiota of supra- and subgingival plaque in health and periodontitis. *J Clin Periodontol* 1999;27:648–57.

5. **Muniz FWMG, De Oliveira CC, De Sousa Carvalho R, Moreira MMSM, De Moraes MEA, *et al.*** Azithromycin: A new concept in adjuvant treatment of periodontitis. *Eur J Pharmacol* 2013;705:135–139.

6. **Colombo AP, Boches SK, Cotton SL, Goodson JM, Kent R, *et al.*** Comparisons of subgingival microbial profiles of refractory periodontitis, severe periodontitis, and periodontal health using the human oral microbe identification microarray. *J Periodontol* 2009;80:1132–1421.

7. **Lohr G, Beikler T, Hensel A**. Inhibition of in vitro adhesion and virulence of Porphyromonas gingivalis by aqueous extract and polysaccharides from Rhododendron ferrugineum L. A new way for prophylaxis of periodontitis? *Fitoterapia* 2015;107:105–113.

8. **Kariu T, Nakao R, Ikeda T, Nakashima K, Potempa J, *et al.*** Inhibition of gingipains and Porphyromonas gingivalis growth and biofilm formation by prenyl flavonoids. *J Periodontal Res* 2016;52:89–96.

9. **Huq NL, Seers CA, Toh ECY, Dashper SG, Slakeski N, *et al.*** Propeptide-Mediated Inhibition of Cognate Gingipain Proteinases. *PLoS One* 2013;8:e65447–e65447.

10. **Dominy SS, Lynch C, Ermini F, Benedyk M, Marczyk A, *et al.*** Porphyromonas gingivalis in Alzheimer's disease brains: Evidence for disease causation and treatment with small-molecule inhibitors . *Sci Adv* 2019;5:eaau3333.

11. **Parker D, Soong G, Planet P, Brower J, Ratner AJ, *et al.*** The NanA neuraminidase of Streptococcus pneumoniae is involved in biofilm formation. *Infect Immun* 2009;77:3722–3730.

12. **Galen JE, Ketley JM, Fasano A, Richardson SH, Wasserman SS, *et al.*** Role of Vibrio cholerae Neuraminidase in the Function of Cholera Toxin. *Infect Immun* 1992;60:406–415.

13. **Stafford G, Roy S, Honma K, Sharma A**. Sialic acid, periodontal pathogens and Tannerella forsythia: Stick around and enjoy the feast! *Mol Oral Microbiol* 2012;27:11–22.

14. **Palmer RJ**. Composition and development of oral bacterial communities. *Periodontol 2000* 2014;64:20–39.

15. **Frey AM, Ansbro K, Kamble NS, Pham TK, Stafford GP**. Characterisation and pure culture of putative health-associated oral bacterium BU063 (Tannerella sp . HOT-286) reveals presence of a potentially novel glycosylated S-layer. FEMS Letters 2018;365:1–8.

16. **Roy S, Honma K, Douglas I, Sharma A, Stafford GP, *et al.*** Role of sialidase in glycoprotein utilisation by Tannerella forsythia. *Microbiology* 2011;157:3195–3202.

17. **Li C, Kurniyati, Hu B, Bian J, Sun J, *et al.*** Abrogation of neuraminidase reduces biofilm formation, capsule biosynthesis, and virulence of Porphyromonas gingivalis. *Infect Immun* 2012;80:3–13.

18. **Aruni W, Vanterpool E, Osbourne D, Roy F, Muthiah A, *et al.*** Sialidase and sialoglycoproteases can modulate virulence in Porphyromonas gingivalis. *Infect Immun* 2011;79:2779–2791.

19. **Kurniyati K, Zhang W, Zhang K, Li C**. A surface-exposed neuraminidase affects complement resistance and virulence of the oral spirochaete Treponema denticola. *Mol Microbiol* 2013;89:842–856.

20. **Duran-Pinedo AE, Chen T, Teles R, Starr JR, Wang X, *et al.*** Community-wide transcriptome of the oral microbiome in subjects with and without periodontitis. *ISME J* 2014;8:1659–72.

21. **Gul SS, Griffiths GS, Stafford GP, Al-Zubidi MI, Rawlinson A, *et al.*** Investigation of a Novel Predictive Biomarker Profile for the Outcome of Periodontal Treatment. *J Periodontol*. Epub ahead of print 2017. DOI: 10.1902/jop.2017.170187.

22. **Honma K, Mishima E, Sharma A**. Role of tannerella forsythia NanH sialidase in epithelial cell

attachment. *Infect Immun* 2011;79:393–401.

23. **Phansopa C, Kozak RP, Liew LP, Frey AM, Farmilo T, *et al.*** Characterization of a sialate-O-acetylesterase (NanS) from the oral pathogen Tannerella forsythia that enhances sialic acid release by NanH, its cognate sialidase. *Biochem J* 2015;472:157–167.

24. **Frey AM, Satur MJ, Phansopa C, Parker JL, Bradshaw D, *et al.*** Evidence for a novel Carbohydrate Binding Module (CBM) of Tannerella forsythia NanH sialidase, key to interactions at the host-pathogen interface. *Biochem J* 2018;20170592:BCJ20170592.

25. **Honma K, Mishima E, Inagaki S, Sharma A**. The OxyR homologue in Tannerella forsythia regulates expression of oxidative stress responses and biofilm formation. *Microbiology* 2009;155:1912–1922.

26. **Royle L, Mattu TS, Hart E, Langridge JI, Merry AH, *et al.*** An analytical and structural database provides a strategy for sequencing O-glycans from microgram quantities of glycoproteins. *Anal Biochem* 2002;304:70–90.

27. **Schindelin J, Arganda-Carreras I, Frise E, Kaynig V, Longair M, *et al.*** Fiji: An open-source platform for biological-image analysis. *Nat Methods* 2012;9:676–682.

28. **Komatsu T, Nagano K, Sugiura S, Hagiwara M, Tanigawa N, *et al.*** E-selectin mediates Porphyromonas gingivalis adherence to human endothelial cells. *Infect Immun* 2012;80:2570–2576.

29. **Varki A, Diaz S**. A Neuraminidase from Streptococcus sanguis That Can Release 0-acetylated Sialic Acids. *J Biol Chem* 1983;258:12465–12471.

30. **Suwannakul S, Stafford GP, Whawell SA, Douglas CWI**. Identification of bistable populations of Porphyromonas gingivalis that differ in epithelial cell invasion. *Microbiology* 2010;156:3052–3064.

31. **Al-Taweel FB, Ian Douglas CW, Whawell SA**. The periodontal pathogen Porphyromonas gingivalis preferentially interacts with oral epithelial cells in S phase of the cell cycle. *Infect Immun* 2016;84:1966–1974.

32. **Dickson MA, Hahn WC, Ino Y, Ronfard V, Wu JY, *et al.*** Human keratinocytes that express hTERT and also bypass a p16(INK4a)-enforced mechanism that limits life span become immortal yet retain normal growth and differentiation characteristics. *Mol Cell Biol* 2000;20:1436–47.

686 33. **Naylor KL, Widziolek M, Hunt S, Conolly M, Hicks M, *et al.*** Role of OmpA2 surface regions of
687 Porphyromonas gingivalis in host – pathogen interactions with oral epithelial cells. *Microbiol*
688 *Open* 2017;1–11.

689 34. **Saito A, Kokubu E, Inagaki S, Imamura K, Kita D, *et al.*** Porphyromonas gingivalis entry into
690 gingival epithelial cells modulated by Fusobacterium nucleatum is dependent on lipid rafts.
691 *Microb Pathog* 2012;53:234–242.

692 35. **Inagaki S, Onishi S, Kuramitsu HK, Sharma A**. Porphyromonas gingivalis vesicles enhance
693 attachment, and the leucine-rich repeat BspA protein is required for invasion of epithelial
694 cells by 'Tannerella forsythia'. *Infect Immun* 2006;74:5023–5028.

695 36. **Kirschbaum M, Schultze-Mosgau S, Pfister W, Eick S**. Mixture of periodontopathogenic
696 bacteria influences interaction with KB cells. *Anaerobe* 2010;16:461–468.

697 37. **Sharma A, Inagaki S, Sigurdson W, Kuramitsu HK**. Synergy between Tannerella forsythia and
698 Fusobacterium nucleatum in biofilm formation. *Oral Microbiol Immunol* 2005;20:39–42.

699 38. **Settem RP, El-Hassan AT, Honma K, Stafford GP, Sharma A**. Fusobacterium nucleatum and
700 tannerella forsythia induce synergistic alveolar bone loss in a mouse periodontitis model.
701 *Infect Immun* 2012;80:2436–2443.

702 39. **Tan KH, Seers CA, Dashper SG, Mitchell HL, Pyke JS, *et al.*** Porphyromonas gingivalis and
703 Treponema denticola Exhibit Metabolic Symbioses. *PLoS Pathog*;10. Epub ahead of print
704 2014. DOI: 10.1371/journal.ppat.1003955.

705 40. **Govinden G, Naylor JLPKL, Anumba AMFDOC, Stafford GP**. Inhibition of sialidase activity and
706 cellular invasion by the bacterial vaginosis pathogen Gardnerella vaginalis. *Arch Microbiol*
707 2018;200:1129–1133.

708 41. **Walther E, Richter M, Xu Z, Kramer C, von Grafenstein S, *et al.*** Antipneumococcal activity of
709 neuraminidase inhibiting artocarpin. *Int J Med Microbiol* 2015;305:289–297.

710 42. **Roy S, Honma K, Ian Douglas CW, Sharma A, Stafford GP**. Role of sialidase in glycoprotein
711 utilization by Tannerella forsythia. *Microbiology* 2011;157:3195–3202.

712 43. **Lewis WG, Robinson LS, Perry J, Bick JL, Peipert JF, *et al.*** Hydrolysis of Secreted
713 Sialoglycoprotein Immunoglobulin A (IgA) in ex Vivo and Biochemical Models of Bacterial. *J*
714 *Biol Chem* 2012;287:2079–2089.

44. **Davey ME, Duncan MJ**. Enhanced Biofilm Formation and Loss of Capsule Synthesis : Deletion of a Putative Glycosyltransferase in Porphyromonas gingivalis. *J Bacteriol* 2006;188:5510–5523.

45. **Bao K, Belibasakis G, Thurnheer T, Aduse-Opoku J, Curtis M *et al***. Role of Porphyromonas gingivalis gingipains in multi-species biofilm formation. *BMC Microbiol* 2014;14:1-8.

46. **Bloch S, Thurnheer T, Murakami Y, Belibasakis G, Schäffer C, *et al*.** Behavior of two Tannerella forsythia strains and their cell surface mutants in multispecies oral biofilms. *Mol Oral Microbiol* 2017;32:5:404-418.

47. **Han YW, Ikegami A, Rajanna C, Kawsar HI, Zhou Y, *et al.*** Identification and Characterization of a Novel Adhesin Unique to Oral Fusobacteria. *J Bacteriol* 2005;187:5330–5340.

48. **Saito A, Inagaki S, Ishihara K**. Differential ability of periodontopathic bacteria to modulate invasion of human gingival epithelial cells by *Porphyromonas gingivalis*. *Microb Pathog* 2009;47:329–333.

49. **Stamatos NM, Carubelli I, van de Vlekkert D, Bonten EJ, Papini N, *et al.*** LPS-induced cytokine production in human dendritic cells is regulated by sialidase activity. *J Leukoc Biol* 2010;88:1227–1239.

50. **Hata K, Koseki K, Yamaguchi K, Moriya S, Suzuki Y, *et al.*** Limited inhibitory effects of oseltamivir and zanamivir on human sialidases. *Antimicrob Agents Chemother* 2008;52:3484–3491.

51. **Amith SR, Jayanth P, Franchuk S, Finlay T, Seyrantepe V, *et al.*** Neu1 desialylation of sialyl α-2,3-linked β-galactosyl residues of TOLL-like receptor 4 is essential for receptor activation and cellular signaling. *Cell Signal* 2010;22:314–324.

52. **Amith SR, Jayanth P, Franchuk S, Siddiqui S, Seyrantepe V, *et al.*** Dependence of pathogen molecule-induced Toll-like receptor activation and cell function on Neu1 sialidase. *Glycoconj J* 2009;26:1197–1212.

Figure legends:

Figure 1. pH optima of *P. gingivalis* whole cell sialidase activity and purified recombinant SiaPG. MUNANA was incubated with SiaPG for 1 minute or *P. gingivalis* (ATCC 33277) for 1 hour, in a variety of buffers with variable pH. Reactions were halted and the pH equalised by addition of an excess of sodium carbonate-bicarbonate buffer, pH 10.5. Sialidase activity catalysed the production of 4-MU from MU-NANA, which was quantified by measuring fluorescence of the reactions at excitation and emission wavelengths of 350 and 450 nm. A) SiaPG (B) *P. gingivalis.* Data shown represent the mean of one experiment where each condition was repeated three times. Error bars = S.E.M.

Figure 2. Reaction kinetics of MUNANA and SiaPG under different conditions. Variable concentrations of MUNANA were exposed to SiaPG, under different pH and salinity conditions. Reactions were quenched by addition of pH 10.5 buffer at 1, 2, and 3 min, and the rate of 4-MU release determined by application of a 4-MU standard curve. A) Michaelis–Menten plot, rate of 4-MU release (V0, µmol MU released min^{-1} mg^{-1} SiaPG), plotted against [MUNANA] (µM) using Prism 7 (GraphPad). Error bars = SD (B) Table summarising Michaelis-Menten reaction kinetics and catalytic efficiency of SiaPG and MU-NANA, the table includes the k_{cat} (4-MU release min^{-1}), and k_{cat}/K_M (µM min^{-1}). Data shown represent the mean (± S.D.) of one experiment, where each condition was repeated three times per experiment.

Figure 3. Reaction kinetics of 3- or 6- sialyllactose and SiaPG under different conditions. Variable concentrations of sialyllactose were exposed to SiaPG, under conditions mimicking physiological (pH 7.4 200 mM NaCl). Reactions were quenched by commencing the thiobarbituric acid assay at 1, 2, and 3 min, and the rate of Neu5Ac release determined by application of a Neu5Ac standard curve. (A) Michaelis–Menten plot, rate of 4-MU release (V0, µmol MU released min^{-1} mg^{-1} SiaPG), plotted against [3- or 6- sialyllactose] (µM) using Prism 7 (GraphPad). Error bars = SEM. (B) Table summarising Michaelis-Menten reaction kinetics and catalytic efficiency of SiaPG and MU-NANA, the table includes the k_{cat} (4-MU release min^{-1}), and k_{cat}/K_M (µM min^{-1}). Data shown represent the mean (± S.D.) of one experiment, where each condition was repeated three times per experiment.

Figure 4. Desialylation of host-relevant glycans by SiaPG. UHPLC chromatogram showing elution of FA2G2S2 and SLeX with and without digestion by SiaPG. FA2G2S2 contains α2-6 linked Neu5Ac. Some contaminating glycans can be observed in the undigested sample, but these also appear to be desialylated. Gc = N-glycolylneuraminic acid. SLeX contains α2-3 linked Neu5Ac.

Figure 6. Inhibition of periodontal pathogen sialidase activity by zanamivir. MUNANA was exposed to periodontal pathogens or purified sialidases. Sialidase activity was expressed as the difference in 4-MU fluorescence relative to conditions with no inhibitor. A) MUNANA was exposed to *T. forsythia* or *P. gingivalis* in the presence of zanamivir for 1 hour and 4 hours, respectively. Data represent the mean of two experimental repeats, where each condition was performed three times per experiment. Error bars = SD. B) MUNANA was exposed to SiaPG and NanH in the presence or absence of zanamivir (1-10 mM, 1 mM increments), and the IC50 of zanamivir for both enzymes obtained using the variable slope model in Graphpad Prism 7. Data represent the mean of three experiments, where each condition was repeated three times. Error bars=SEM.

Figure 7. Enzyme synergy in sialic acid release from BSM, and inhibition by zanamivir. BSM was incubated with either NanS, SiaPG, or NanS + SiaPG, in the presence or absence of 0.5 mM zanamivir, before undergoing the TBA assay to assess sialic acid release. Data based on the mean of three experiments, each condition was tested in triplicate during each experiment. Error Bars=SEM. Significance determined by one-way ANOVA with repeated measures, with Bonferroni correction for multiple comparisons (*p=<0.05, **p=<0.01).

Figure 8. Zanamivir inhibits *P. gingivalis* growth and biofilm formation on sialoglycoproteins. Bacteria were cultured for 5 days at 37 °C anaerobically, in the presence of Neu5Ac, or on surfaces coated with the glycoproteins mucin, saliva, or serum. All conditions were performed in the presence or absence of zanamivir. A) Total growth; OD_{600} of the culture was used to quantify bacteria in both biofilm and planktonic states. B) Biofilm formation, quantified by resuspension of biofilms and counting the number of bacteria under microscopy. All data shown represent the mean of three biological repeats, where conditions were tested three times per experiment. Error bars =SEM. Significance determined by T-test, **p=>0.01, ***p=>0.005.

Figure 9. Biofilm formation by *P. gingivalis* 381, sialidase deficient Pg381ΔsiaPG, and SiaPG complemented strain ΔsiaPG^{+}. *P. gingivalis* strains were resuspended to an OD_{600} 0.5, and seeded into microtitre plates precoated with mucin (BSM), and biofilms were cultured for 24 hours at 37°C anaerobically. Data represent the mean of four replicates per condition. Error bars = SD, statistical significance determined by unpaired T-test compared to the WT strain, **p=<0.01).

Figure 10. Purified sialidases desialylate oral epithelial cell surfaces, and in the case of SiaPG this is inhibited by zanamivir. Cells were stained with lectins for α2-3 and α2-6 linked sialic acid in red and green, respectively. Prior to staining, cells were treated with NanH and SiaPG in PBS, in the presence or absence of 10 mM zanamivir (zan), as indicated. All images were visualised using the same

microscopy and image processing parameters (fluorescence intensity, exposure time and background subtraction). Images were captured in three fields of view, and this was repeated in three separate experiments. Images shown are representative of each condition. Separate colour channels are displayed in the supplementary information (supplemental figure S3).

Figure 11. The effect of zanamivir on attachment and invasion of epithelial cells during monospecies infection. Antibiotic protection assays on OKF6 and H357 cell lines were performed in the presence or absence of 10 mM zanamivir (thatched and black bars, respectively) with either A) *T. forsythia*, B) *P. gingivalis*, or C) *F. nucleatum*. Bacterial attachment, invasion, and total association with host cells was normalised to the number of bacteria that were used to infect each condition that had survived the duration of the assay (the percentage of viable bacteria). Data represent the mean from three independent experimental repeats, and each condition was repeated in triplicate during each experiment. Error bars=SEM, Significance determined by paired T-test, *p=<0.05, **

Figure 12. The effect of zanamivir on attachment and invasion of epithelial cells during multispecies infection. Antibiotic protection assays were performed in the presence or absence of 10 mM zanamivir (thatched and black bars, respectively) with different combinations of *T. forsythia, F. nucleatum,* and *P. gingivalis* to establish host cell association in each instance. A) *T. forsythia* + *F. nucleatum* B) *T. forsythia* + *P. gingivalis.* C) *F. nucleatum* + *P. gingivalis* D) *T. forsythia, F. nucleatum,* and *P. gingivalis.* Bacterial attachment, invasion, and total association with host cells was normalised to the number of bacteria that were used to infect each condition that had survived the duration of the assay (the percentage of viable bacteria). Zanamivir = 10 mM zanamivir present during host cell exposure to bacteria. Data represent the mean from three experimental repeats, and each condition was repeated in triplicate during each experiment. Error bars=SEM, Significance determined by paired T-test, *p=<0.05, **p=<0.01. ***p=<0.001.

831 **Table 1. List of primers used in this study**

832

Primers for *siaPG* deletion mutant	
Primer	Sequence (5'>3')
#1	TACGGCATCGCGGTTTTGA
#2	TCGCCATAGAATACAGGATAAGC
#3	gggcaatttctttttttgtcatTGAAAACTATTTTATACCATTTTGGGA
#4	TCCCAAAATGGTATAAAATAGTTTTCAatgacaaaaaagaaattgccc
#5	aaaaatttcatccttcgtagGAATAGTGCTTTTTTTATCGAGTTTTTC
#6	GAAAAACTCGATAAAAAAAAGCACTATTCctacgaaggatgaaattttt
Sequences in upper case correspond to *siaPG* and lower case to *ermF*.	
Primers for *siaPG* complementation	
FWD BamHI	CGCGGATCCG taatacgactcactatagg
REV SalI	TTGACGTCGACGCGTctagttattgctcagcggtgg
Endonuclease sites are underlined.	

833

Figure 1

Click here to access/download;Figure;Figure 1.jpg

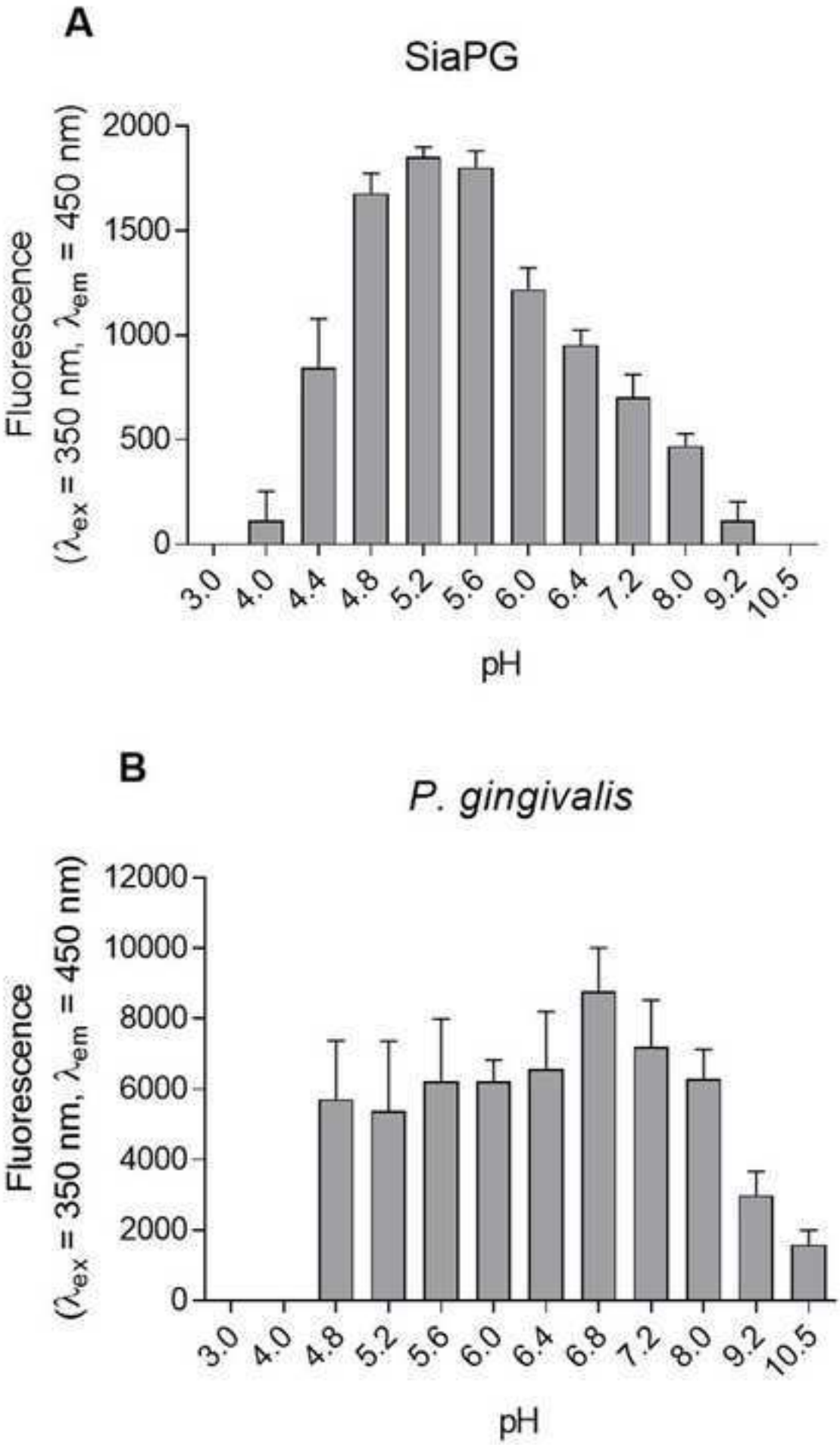

Figure 2

A

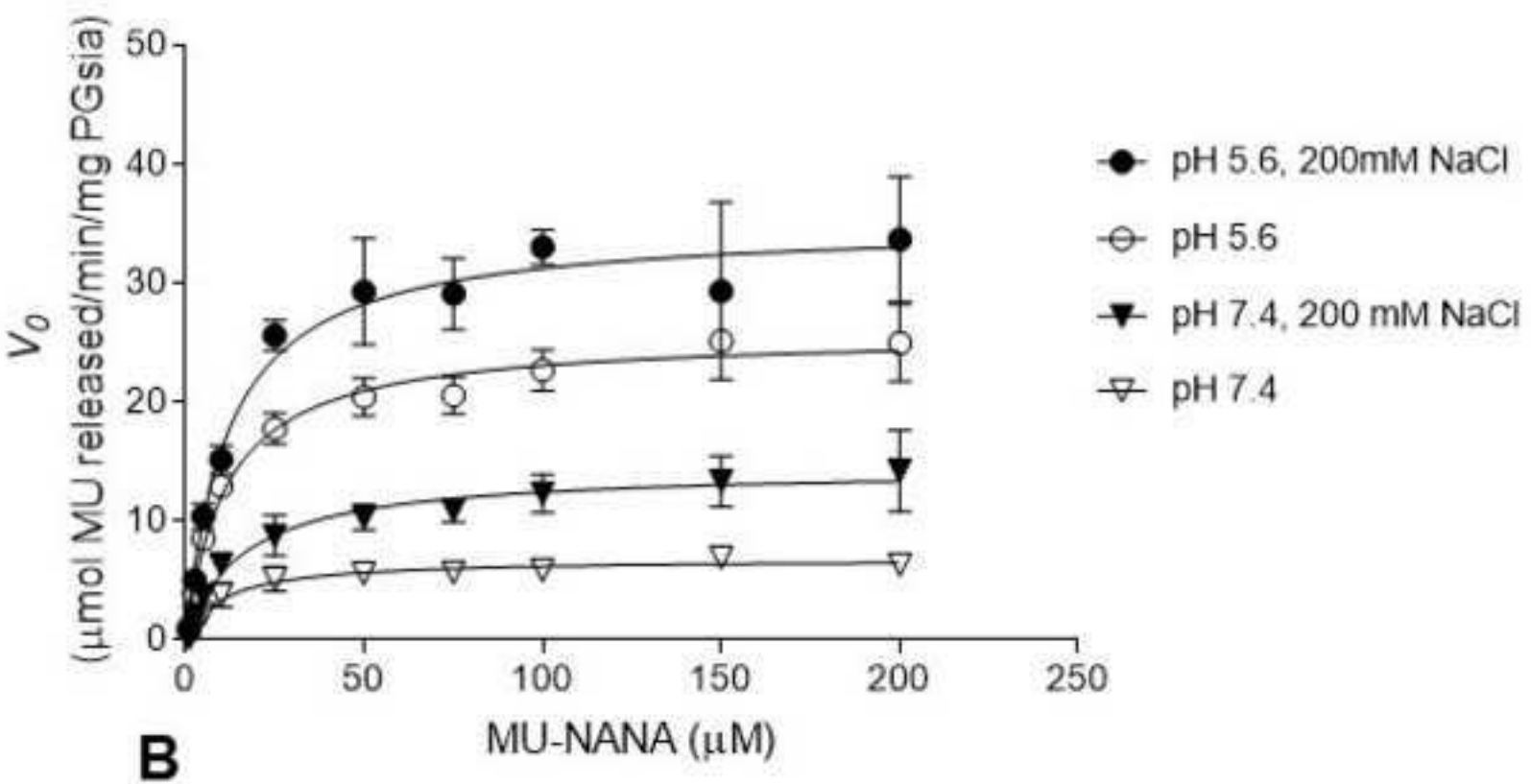

B

	pH 7.4, 200 mM NaCl	pH 7.4	pH 5.6, 200 mM NaCl	pH 5.6
k_{cat} (4-MU release/min)	789.8 ± 43.6	374.8 ± 16.3	1916 ± 69.46	1408 ± 33.28
K_M ([MU-NANA], µM)	15.8 ± 3.7	10.3 ± 2.1	11.9 ± 1.9	11.3 ± 1.2
k_{cat}/K_M (µM/min)	49.9	36.4	161.0	124.7
V_{max} (4-MU release, µmol/min/mg NanH)	14.4 ± 0.8	6.8 ± 0.3	35.0 ± 1.3	25.7 ± 0.6

Figure 3

A

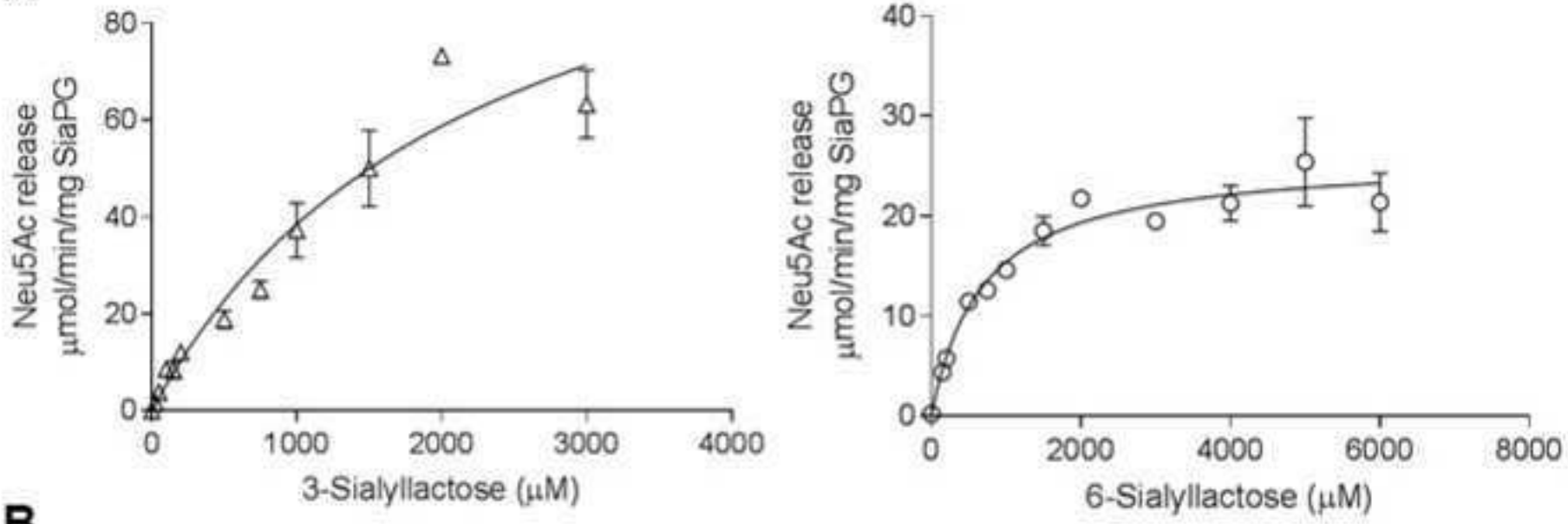

B

	3-Sialyllactose	6-Sialyllactose
K_{cat} (Neu5Ac release/min)	356.8 ± 49.64	74.42 ± 2.8
K_M ([Sialyllactose], uM)	2234 ± 548.8	684.9 ± 92.6
K_{cat}/K_M (uM/min)	0.16	0.11
V_{max} (Neu5ac release, umol/min/mg SiaPG)	124.3 ± 17.3	25.9 ± 1.0

Figure 4

Click here to access/download;Figure;Figure 4.jpg

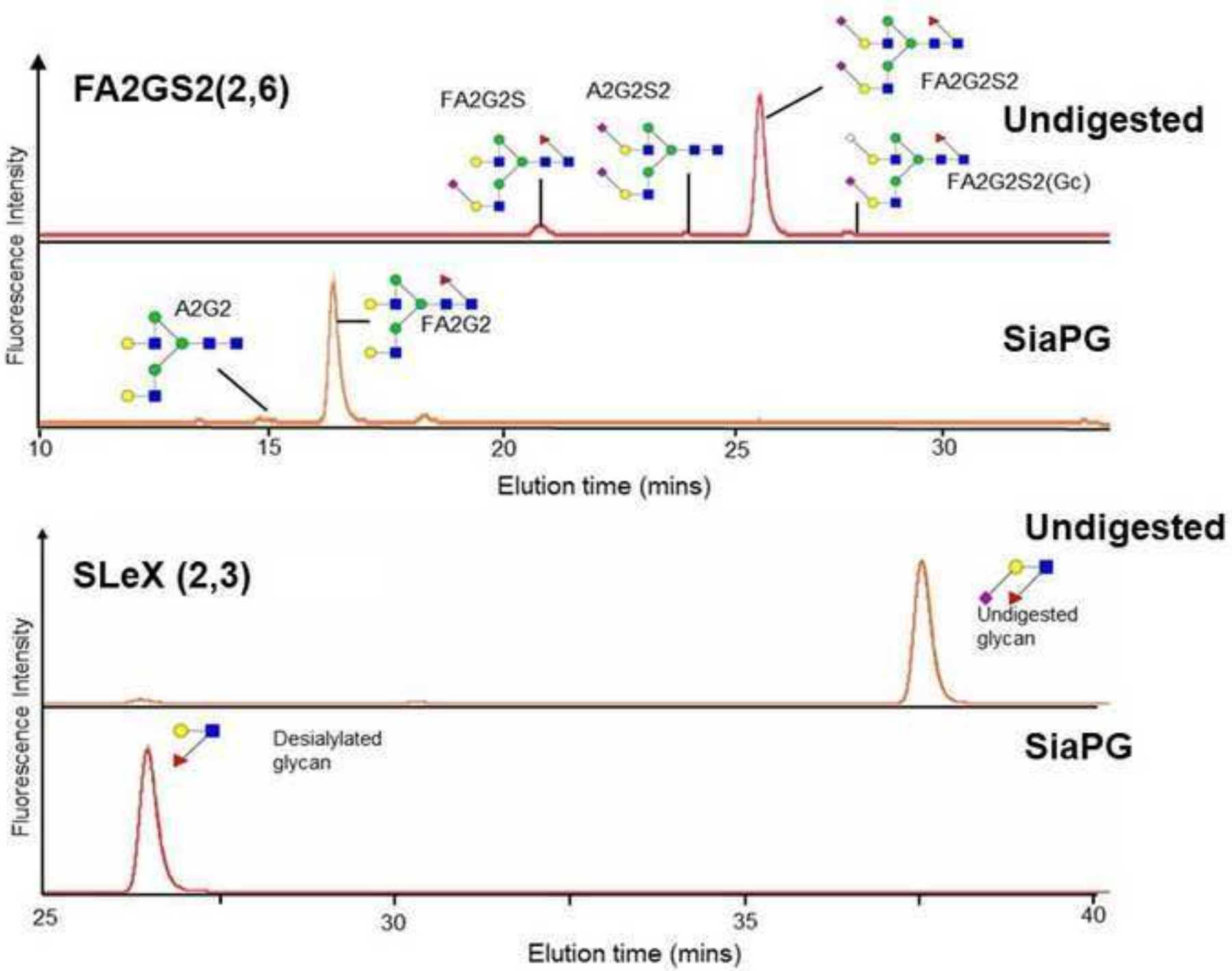

Figure 5

Click here to access/download;Figure;Figure 5.jpg

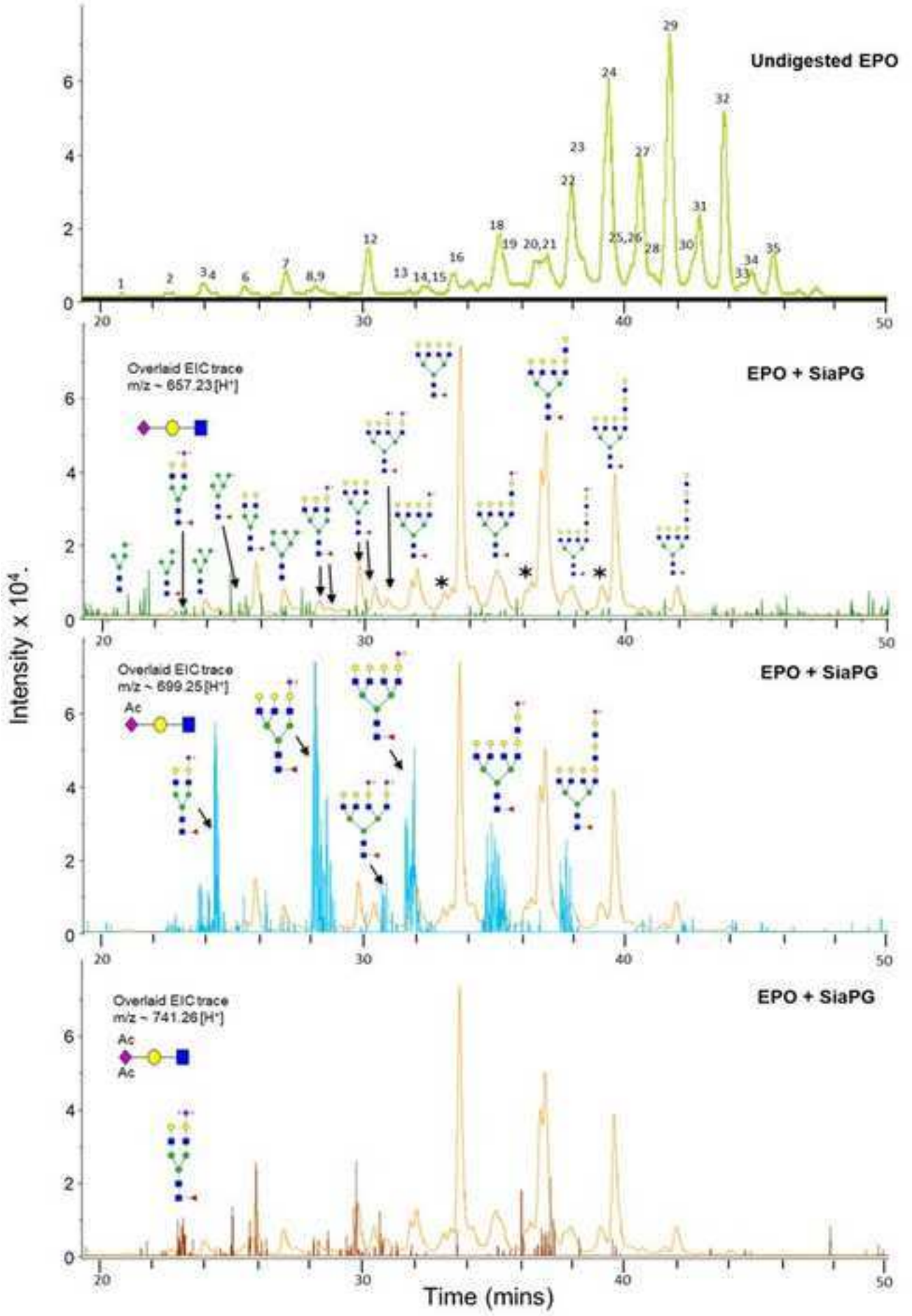

Figure 6

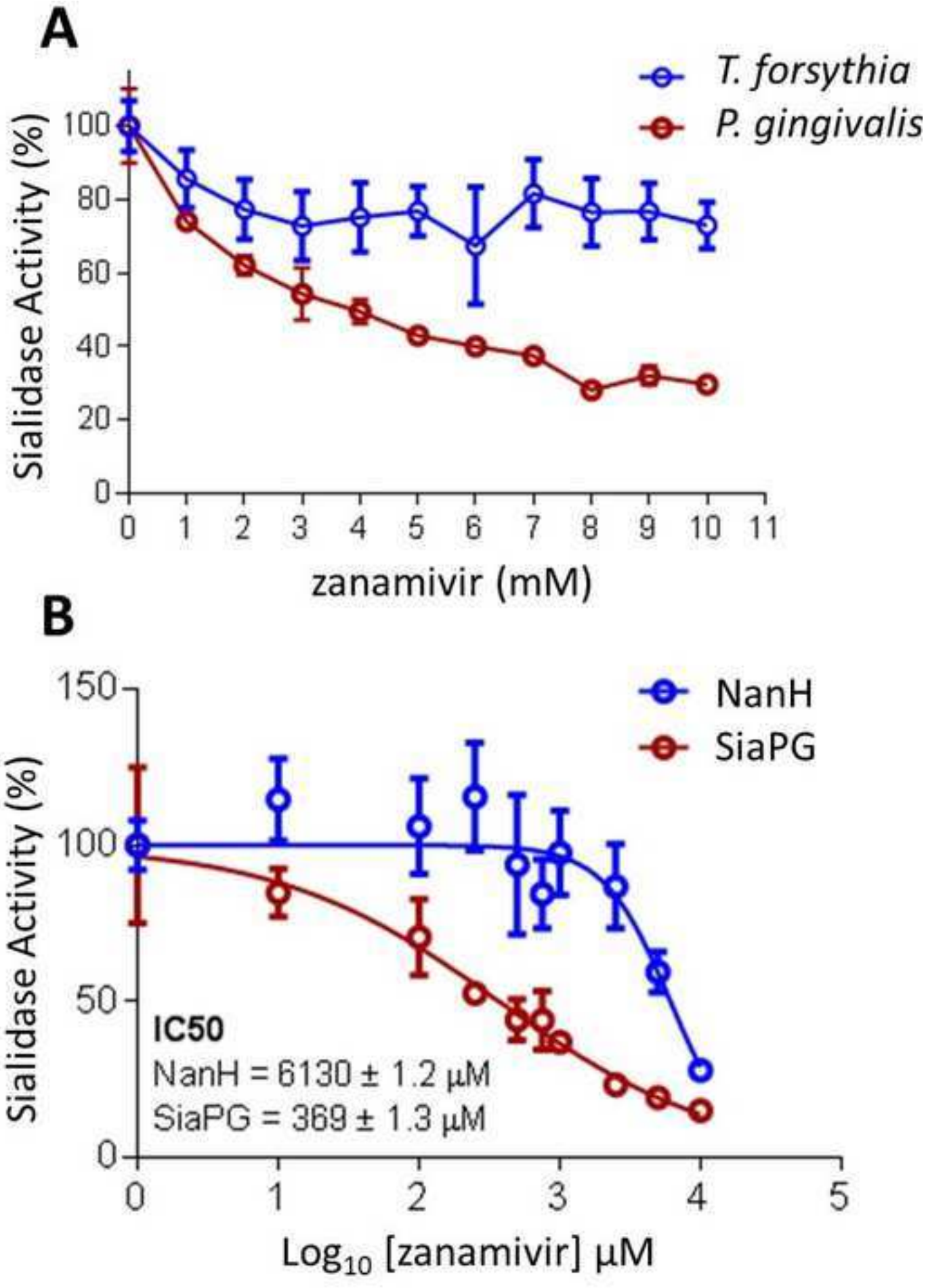

Figure 7

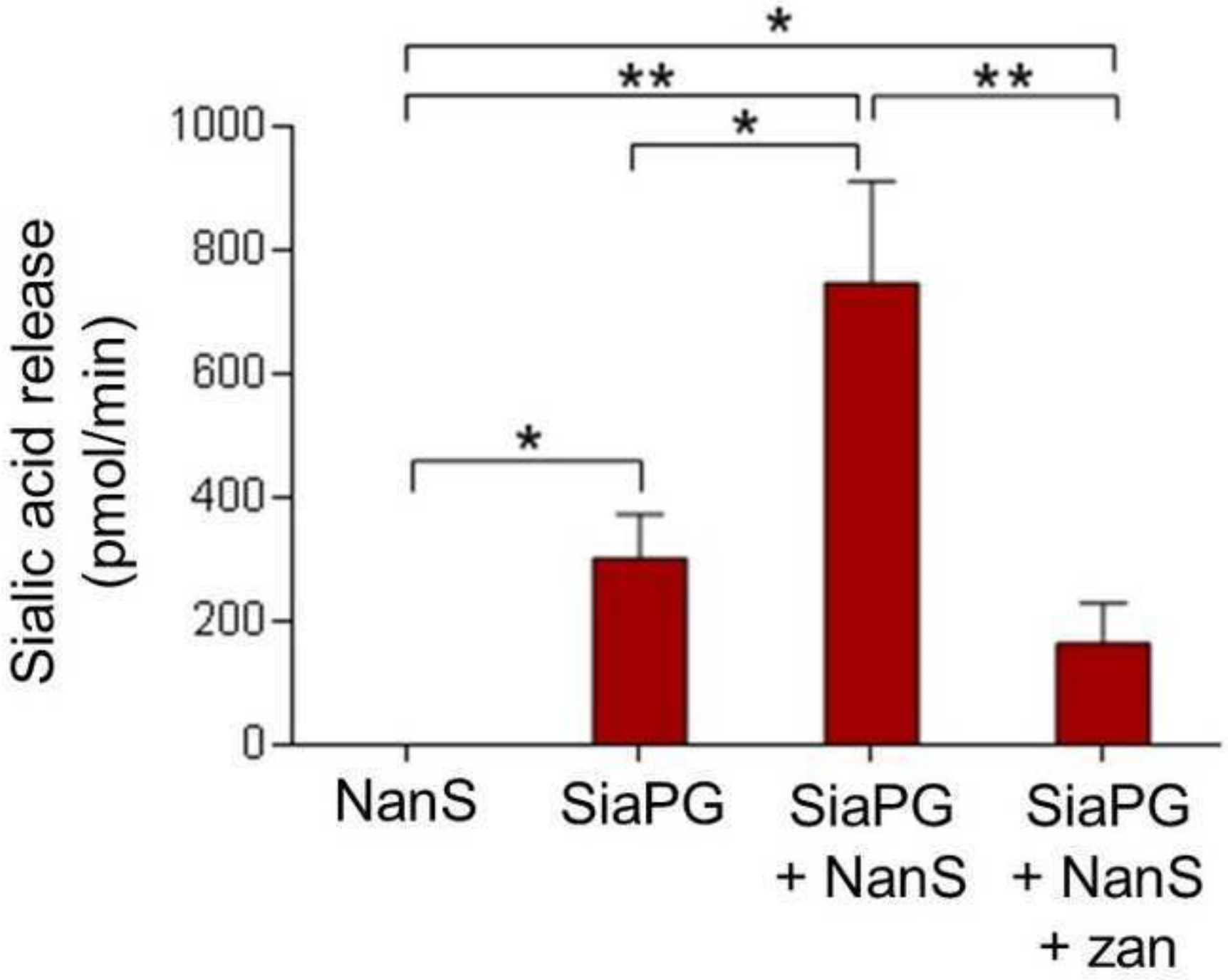

Figure 8

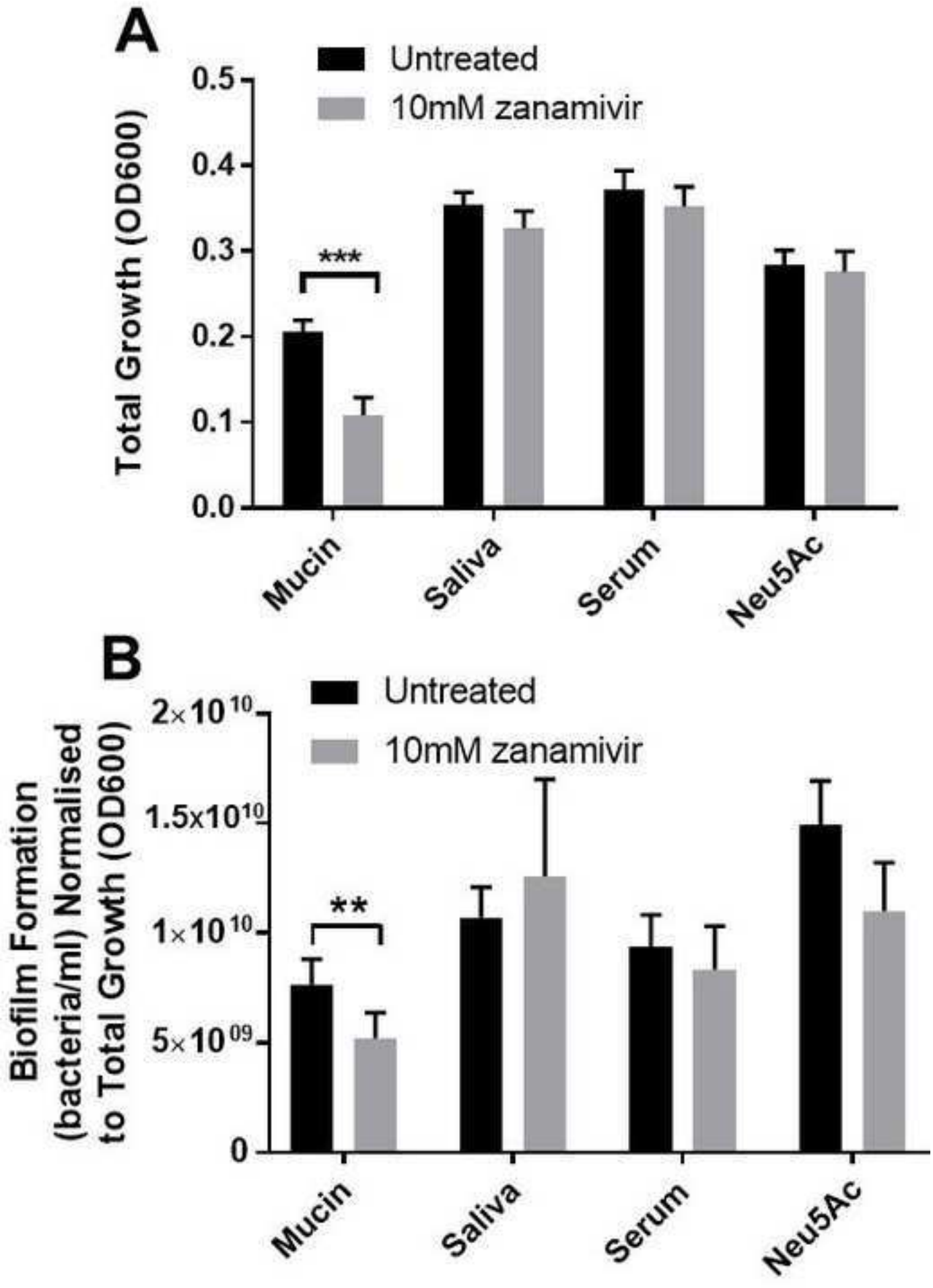

Figure 9

Click here to access/download;Figure;Figure 9.jpg

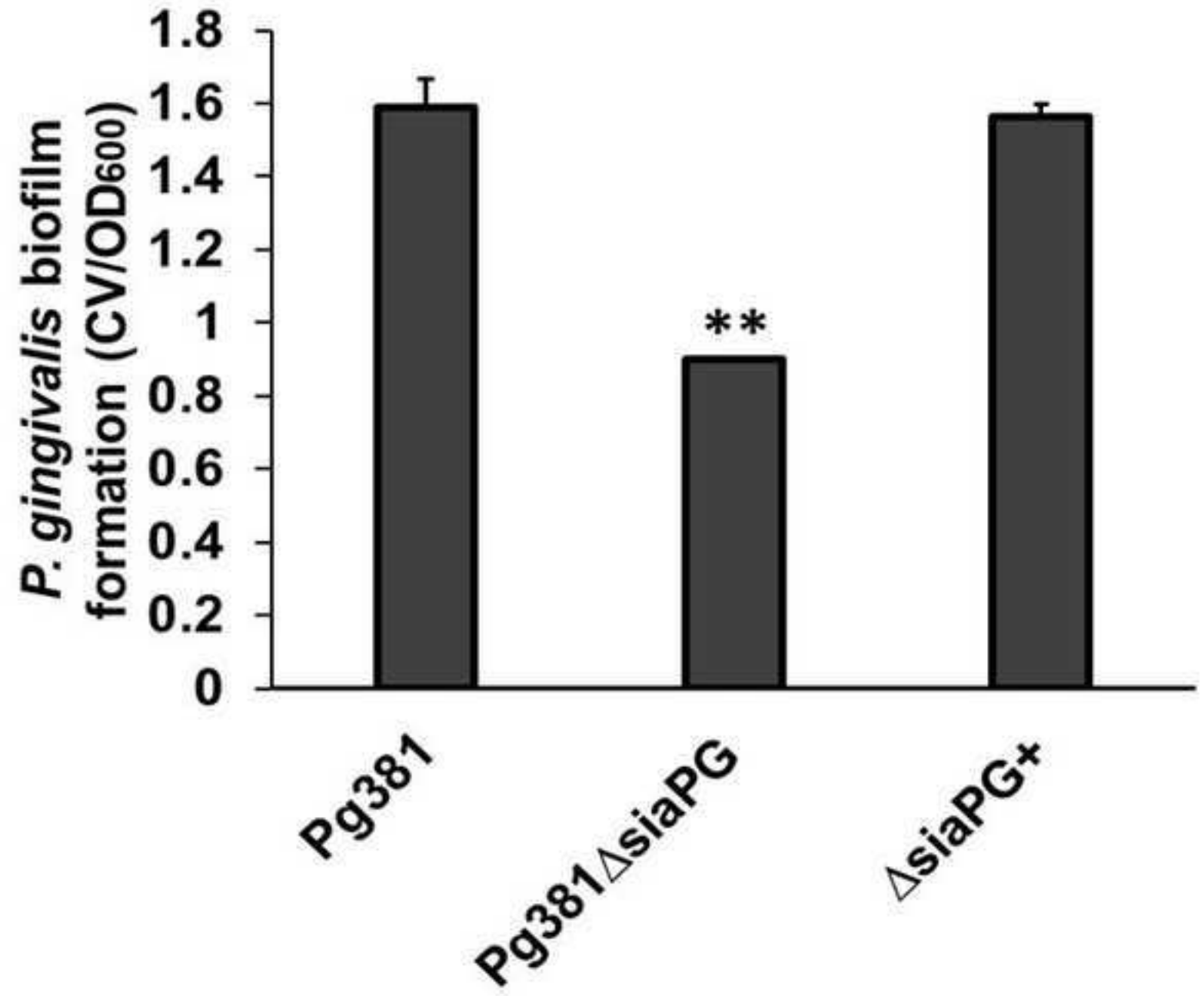

Figure 10

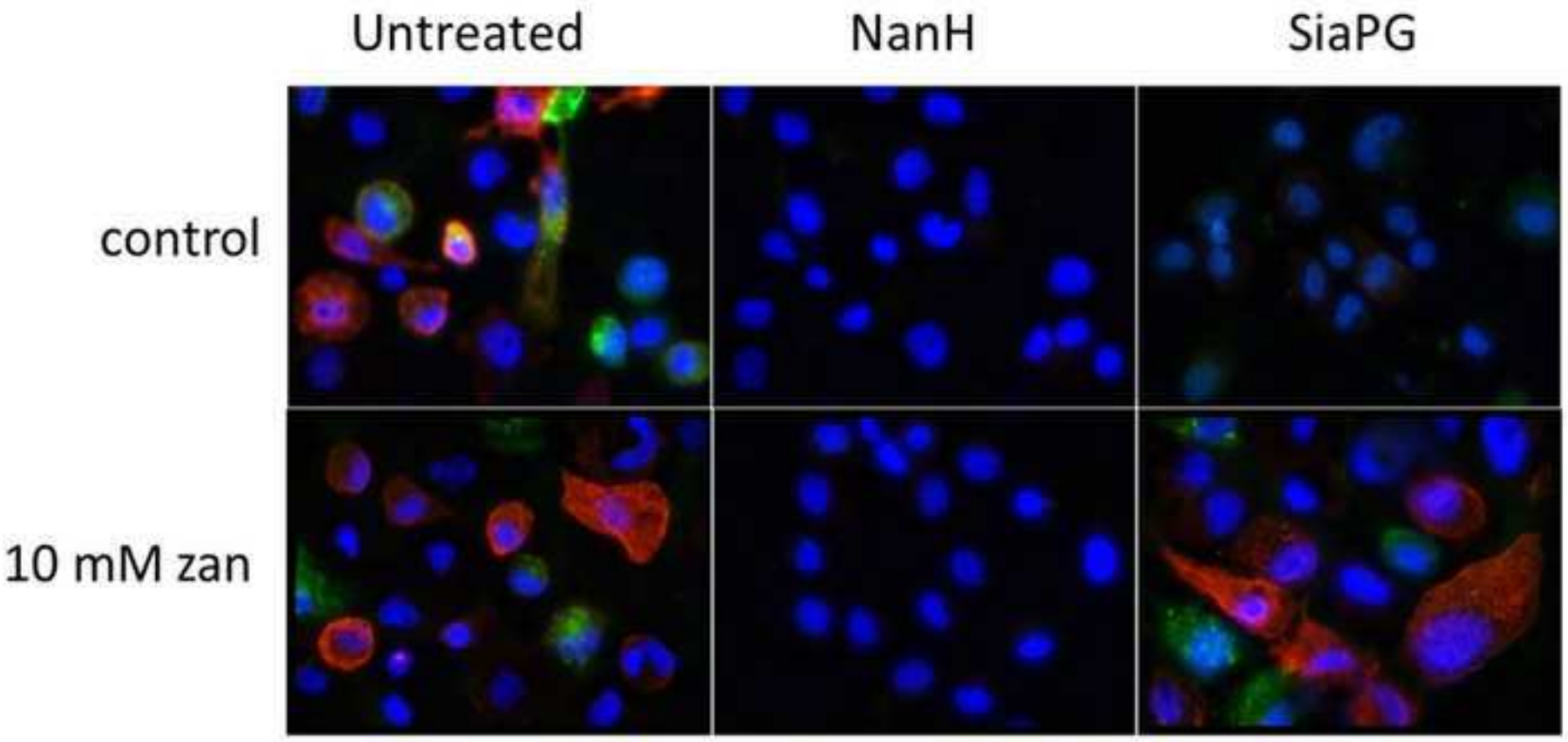

Figure 11

Click here to access/download;Figure;Figure 11.jpg

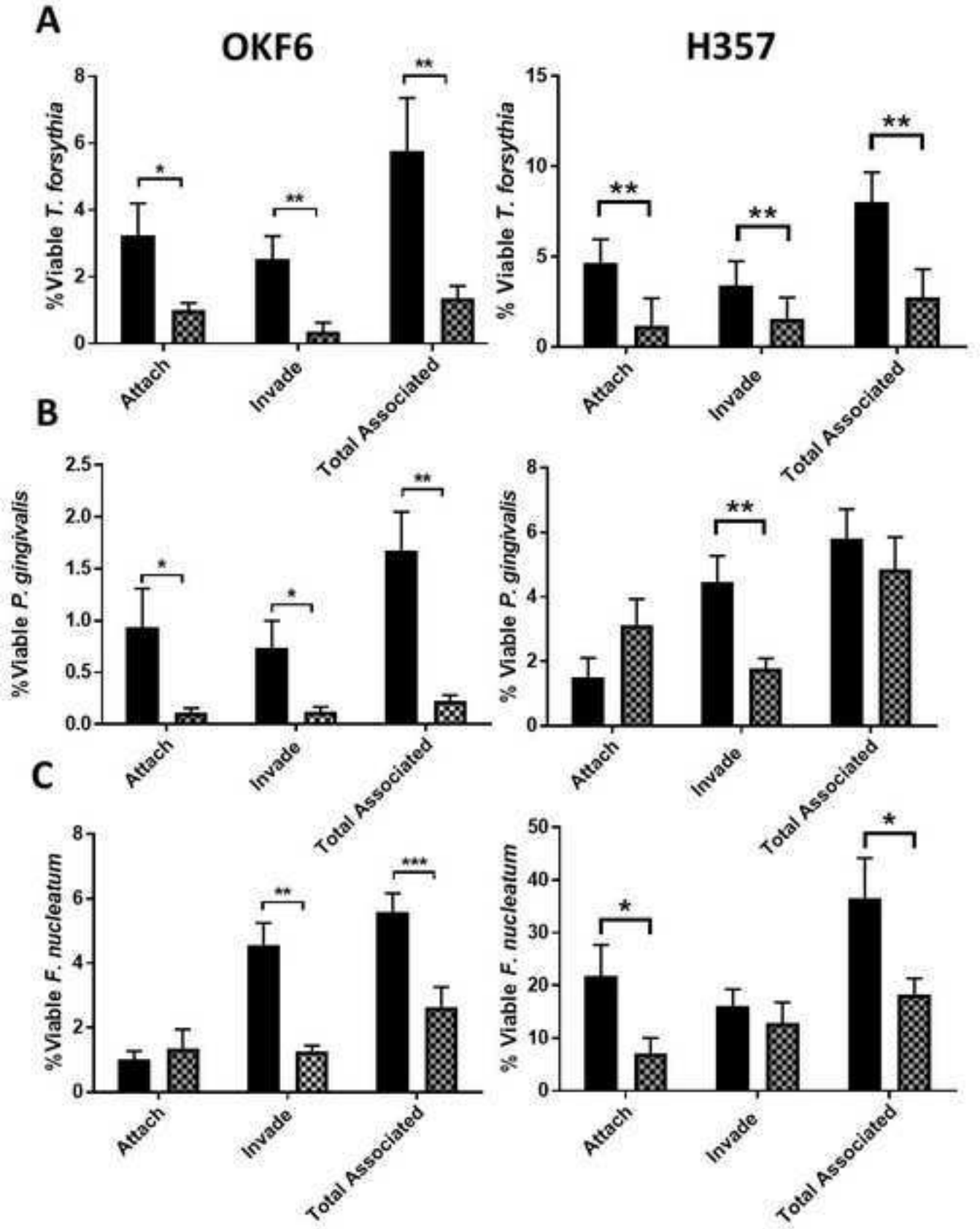

Figure 12

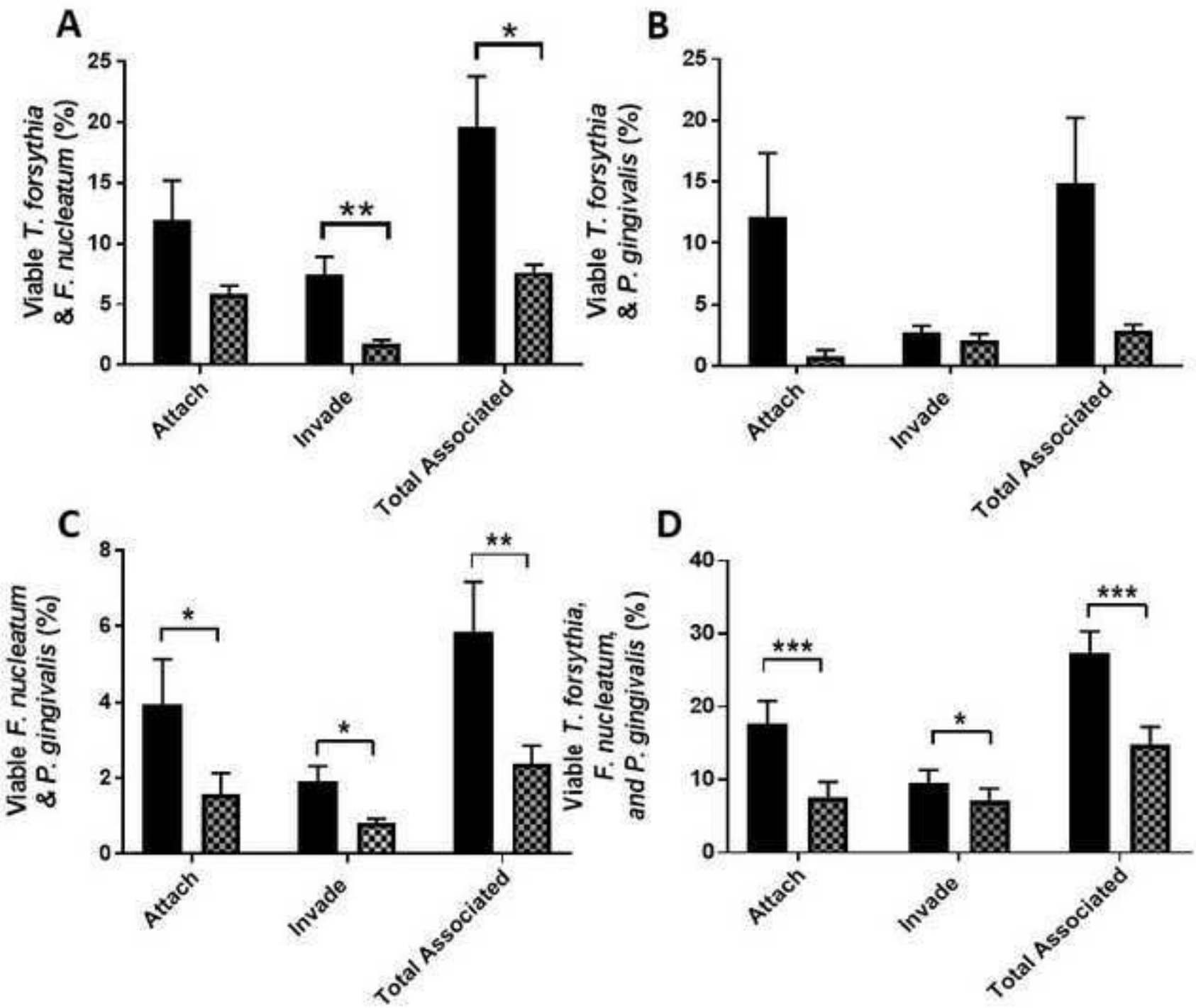

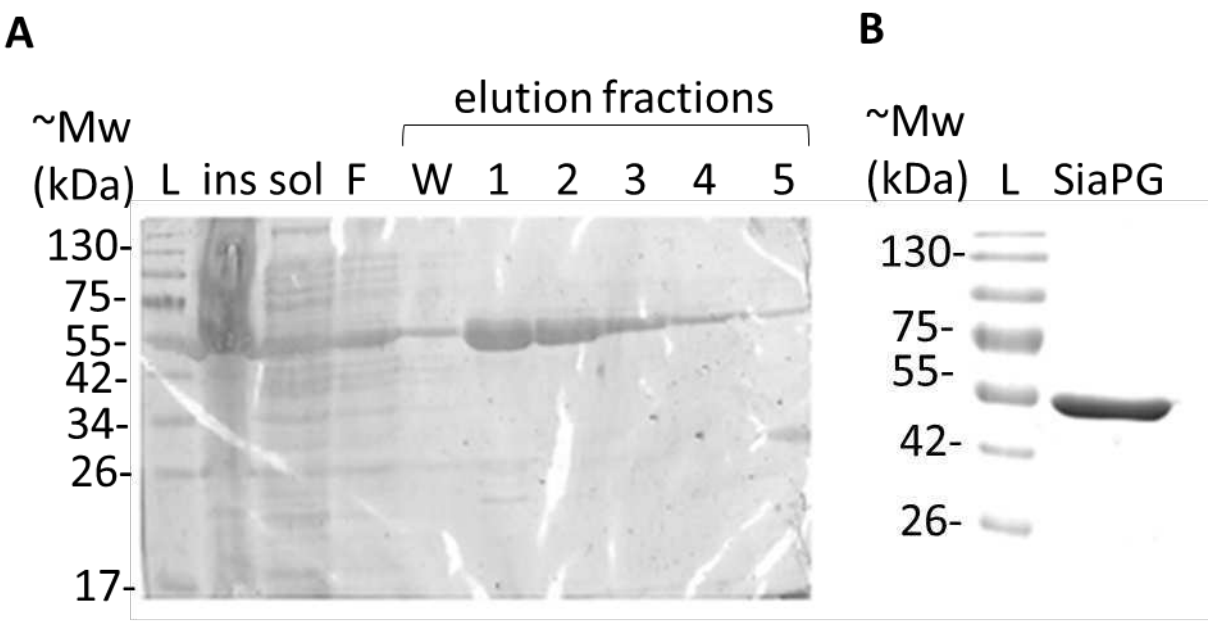

C

Native protein

MANNTLLAKTRRYVCLVVFCCLMAMMMHLSGQEVTMWGDSHGVAPNQVRRTLVKVALSESLPPGAKQIRIGFSLP
KETEEKVTALYLLVSDSLAVRDLPDYKGRVSYDSFPISKEDRTTALSADSVAGRCFFYLAADIGPVASFSRSDTLTARVE
ELAVDGRPLPLKELSPASRRLYREYEALFVPGDGGSRNYRIPSILKTANGTLIAMADRRKYNQTDLPEDIDIVMRRST
DGGKSWSDPRIIVQGEGRNHGFGDVALVQTQAGKLLMIFVGGVGLWQSTPDRPQRTYISESRDEGLTWSPPRDI
THFIFGKDCADPGRSRWLASFCASGQGLVLPSGRVMFVAAIRESGQEYVLNNYVLYSDDEGGTWQLSDCAYHRG
DEAKLSLMPDGRVLMSVRNQGRQESRQRFFALSSDDGLTWERAKQFEGIHDPGCNGAMLQVKRNGRNQMLHS
LPLGPDGRRDGAVYLFDHVSGRWSAPVVVNSGSSAYSDMTLLADGTIGYFVEEDDEISLVFIRFVLDDLFDARQ

Supplemental figure S1. Purification of SiaPG A) SiaPG purification via affinity chromatography. L= Molecular mass ladder, ins = insoluble fraction of whole bacterial lysate, sol = soluble fraction of whole bacterial lysate, F = flow through, W = wash, elution fractions were 1 ml each. B) Purified SiaPG post-dialysis. C) Native gene encoding SiaPG and resulting encoded protein (PG_0352, obtained from UniProt; Q7MX62), 100 % protein identity between W83 and ATCC 33277 strains). Red = secretion signal site, absent in the codon optimized protein expressed here using *E. coli*.

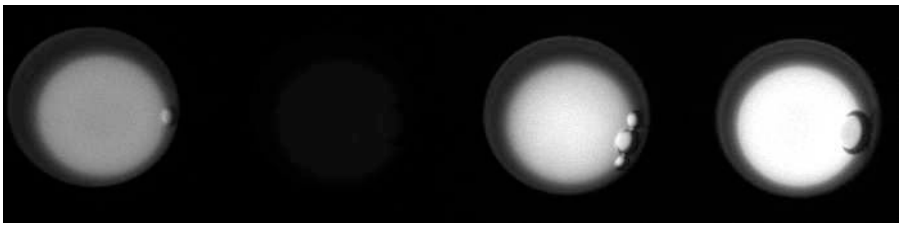

Pg381 Pg381 ΔsiaPG SiaPG ΔsiaPG^{+}

Supplemental figure S2: Sialidase activity of SiaPG, *P. gingivalis* SiaPG-inactivated isogenic mutant (Pg381ΔsiaPG) and its complemented strain (ΔsiaPG^{+})

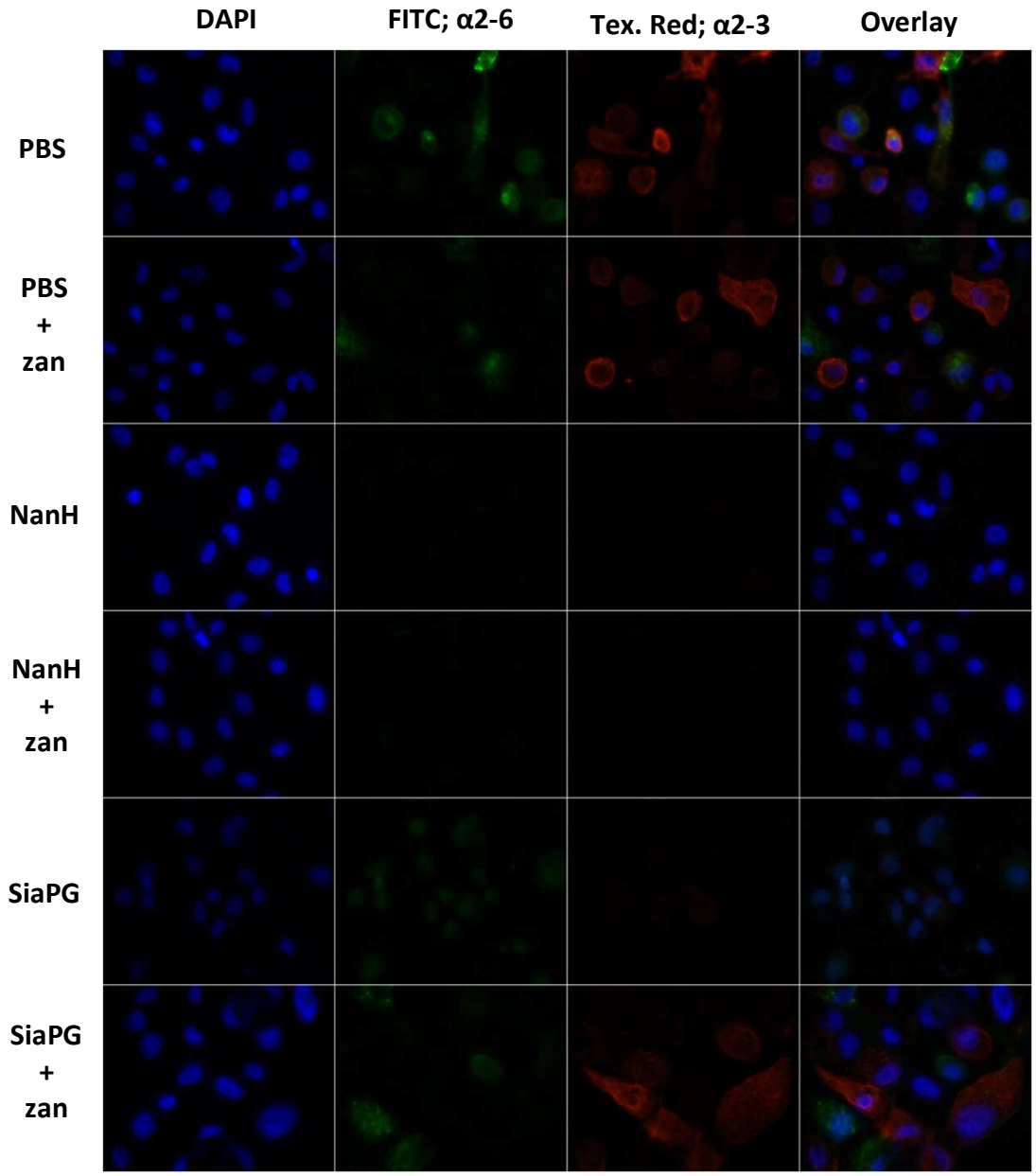

Supplemental figure S3. Purified sialidases desialylate oral epithelial cell surfaces.

Cells were stained with lectins for α2-3 and α2-6 linked sialic acid in red and green, respectively. Prior to staining, cells were treated with NanH and SiaPG in PBS, in the presence or absence of 10mM zanamivir, as indicated. All images were visualised using the same microscopy and image processing parameters (fluorescence intensity, exposure time and background subtraction). Images were captured in three fields of view, and this was repeated in three separate experiments. Images shown are representative of each condition.

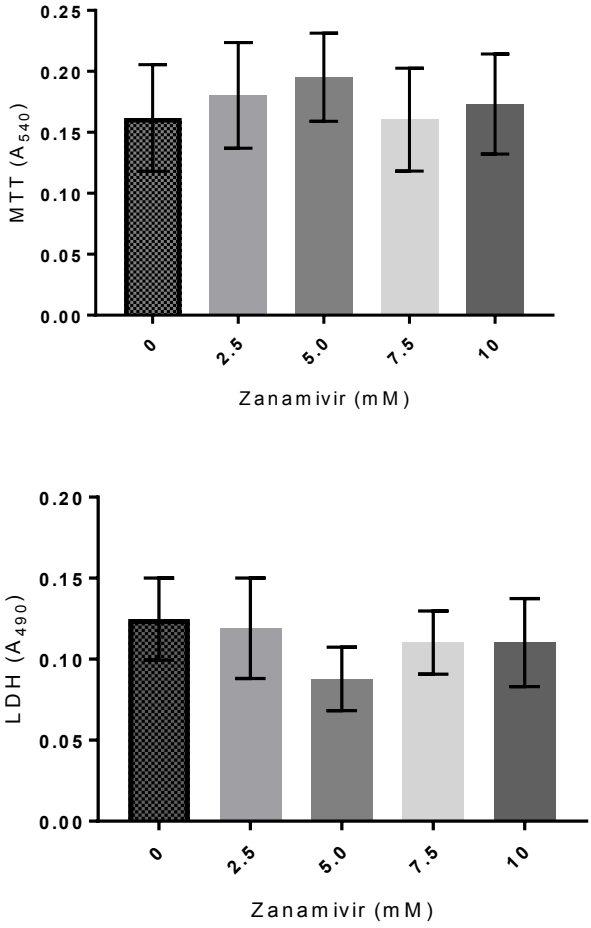

Supplemental figure S4. Viability testing of OKF6 oral epithelial cells exposed to zanamivir.

The oral epithelial cell line OKF6 was exposed to *T. forsythia* in the presence and absence of 10 mM zanamivir for 2.5 hours, followed by an MTT assay on cells, or an LDH assay on culture supernatant, with the absorbance at 490 and 540 nm for LDH and MTT, respectively, used to relatively quantify levels of MTT and LDH. Data shown represent the mean of two experiments, where each condition was repeated three times per experiment. Error bars=SEM. No significant differences were found (where p=<0.05), as determined by one way ANOVA, with repeated measures and Tukey's correction for multiple comparisons.

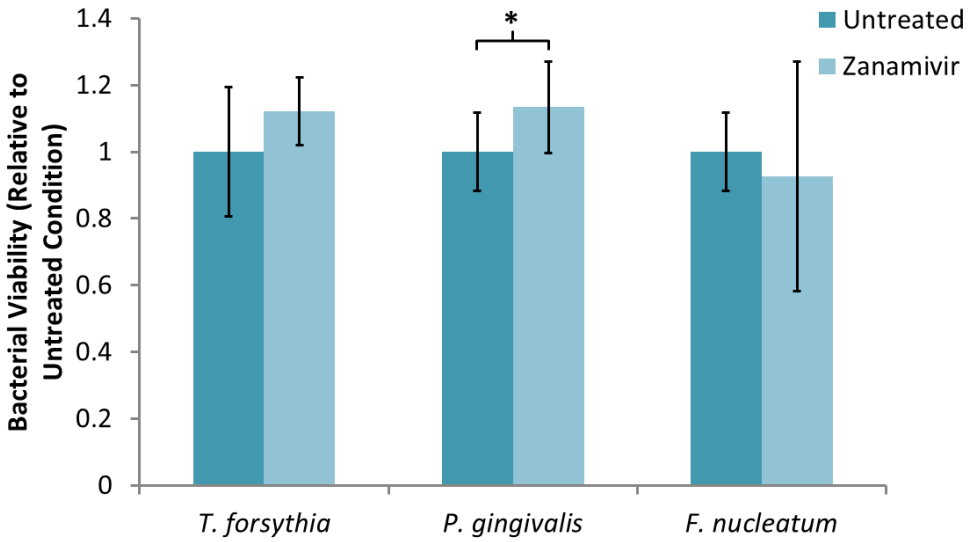

Supplemental figure S5. Viability testing of periodontal pathogens exposed to zanamivir.

T. forsythia, P. gingivalis, and F. nucleatum were incubated in the presence and absence of 10mM zanamivir for 2.5 hours, followed by enumeration of viable organisms by agar plate counts, and data were expressed as the change in cell numbers relative to the untreated condition. Data shown represent the mean of three experiments, where each condition was repeated three times per experiment. Error bars=SD. Significance determined by T-test (*p=<0.05).

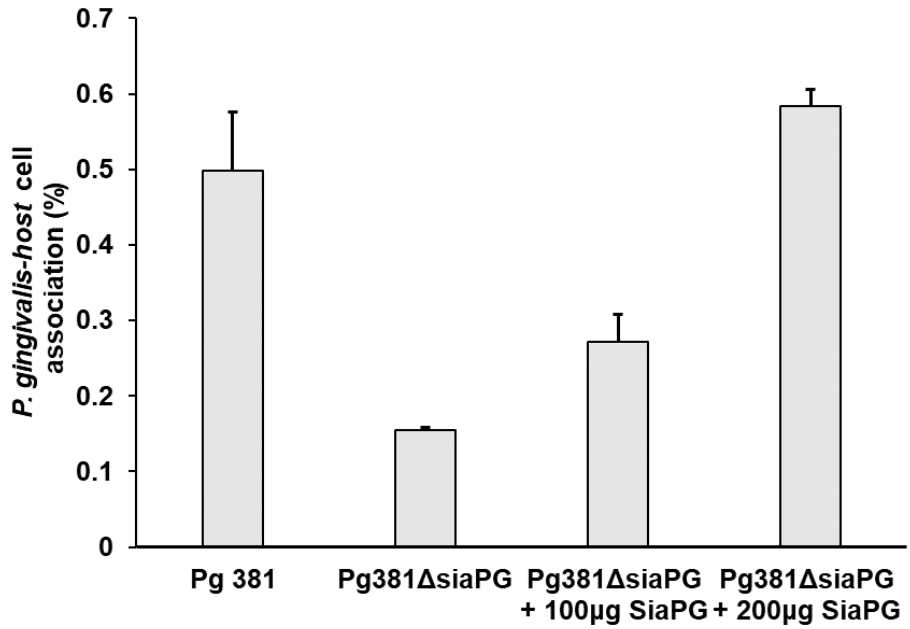

Supplemental Figure S6. Association of *P. gingivalis* with OBA9 cells. OBA-9 cells were incubated with P. gingivalis 381 or the SiaPG inactivated mutant (ΔPG352), in the presence or absence of 100 and 200 µg of SiaPG. Bacterial association was calculated as percentage of input bacteria. Data represent the mean of two experiments, where each condition was repeated three times per experiment. Error bars = SEM, significant differences between Pg 381 and the other conditions were determined by paired T-test, *p=<0.05, **p=<0.01).

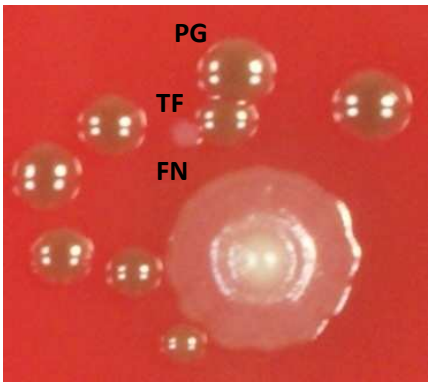

Supplemental figure S7. Colony morphology of *P. gingivalis*, *F. nucleatum*, and *T. forsythia* during mixed-species enumeration.

Images of mixed-species agar cultures to highlight differences in colony morphology. Left panel = unassisted view, right panel = colony counter microscope view. One colony representative of each species is labelled on the images. *P. gingivalis* (PG) forms opaque black-pigmented colonies, *T. forsythia* (TF) forms translucent grey colonies, and *F. nucleatum* (FN) forms large beige colonies, translucent at the edges with a raised, opaque centre.

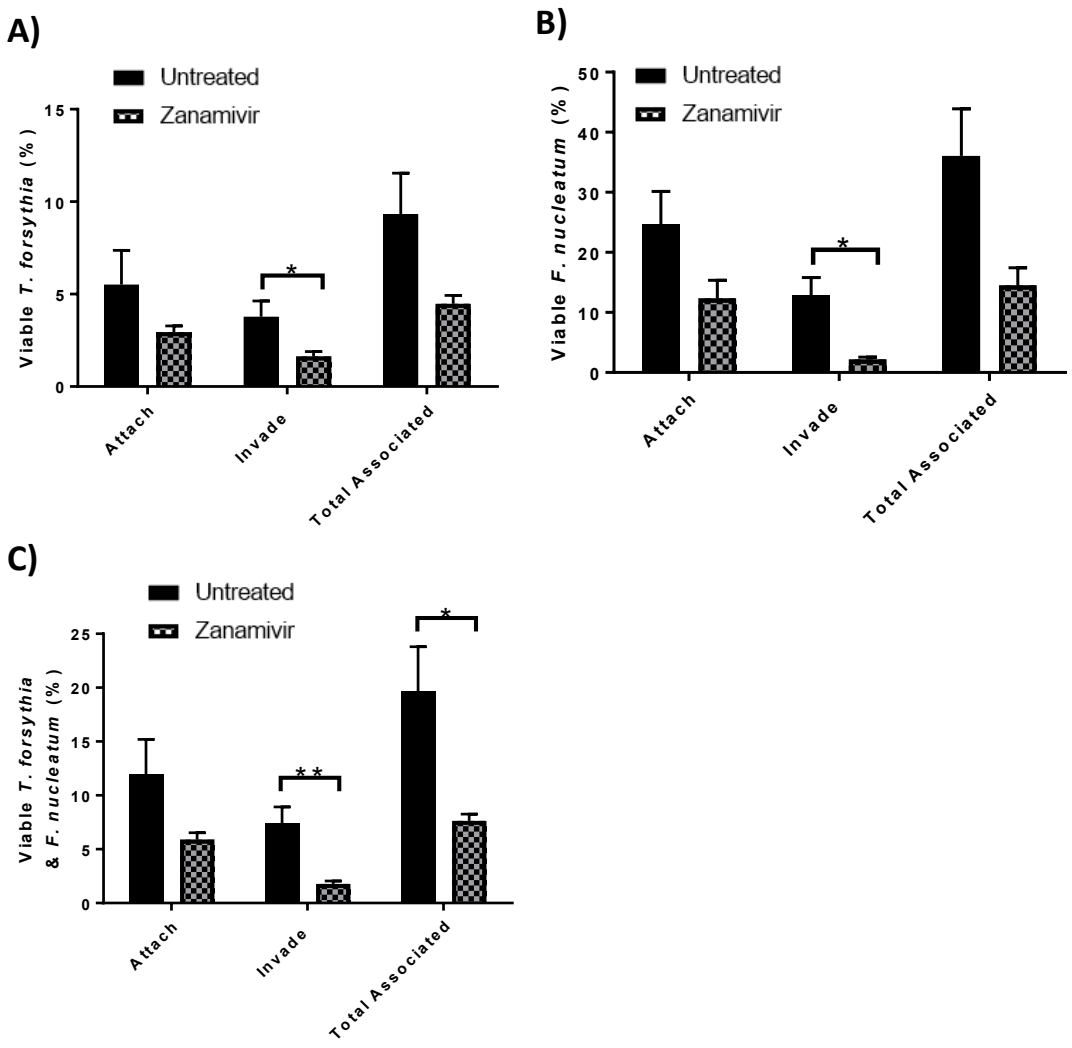

Supplemental figure S8. The effect of zanamivir on attachment and invasion of epithelial cells co-infected with *T. forsythia* and *F. nucleatum*.

Antibiotic protection assays were performed in the presence or absence of zanamivir with *T. forsythia* and *F. nucleatum.* A) Level of *T. forsythia*-host cell association, B) Level of *F. nucleatum*-host cell association, or C) Level of both *T. forsythia* and *F. nucleatum*-host cell association. Bacterial attachment, invasion, and total association with host cells was normalised to the number of bacteria that were used to infect each condition that had survived the duration of the assay (the percentage of viable bacteria). Zanamivir= 10mM zanamivir present during host cell exposure to bacteria. Data represent the mean from three experimental repeats, and each condition was repeated in triplicate during each experiment. Error bars=SEM, Significance determined by paired T-test, *p=<0.05, **p=<0.01.

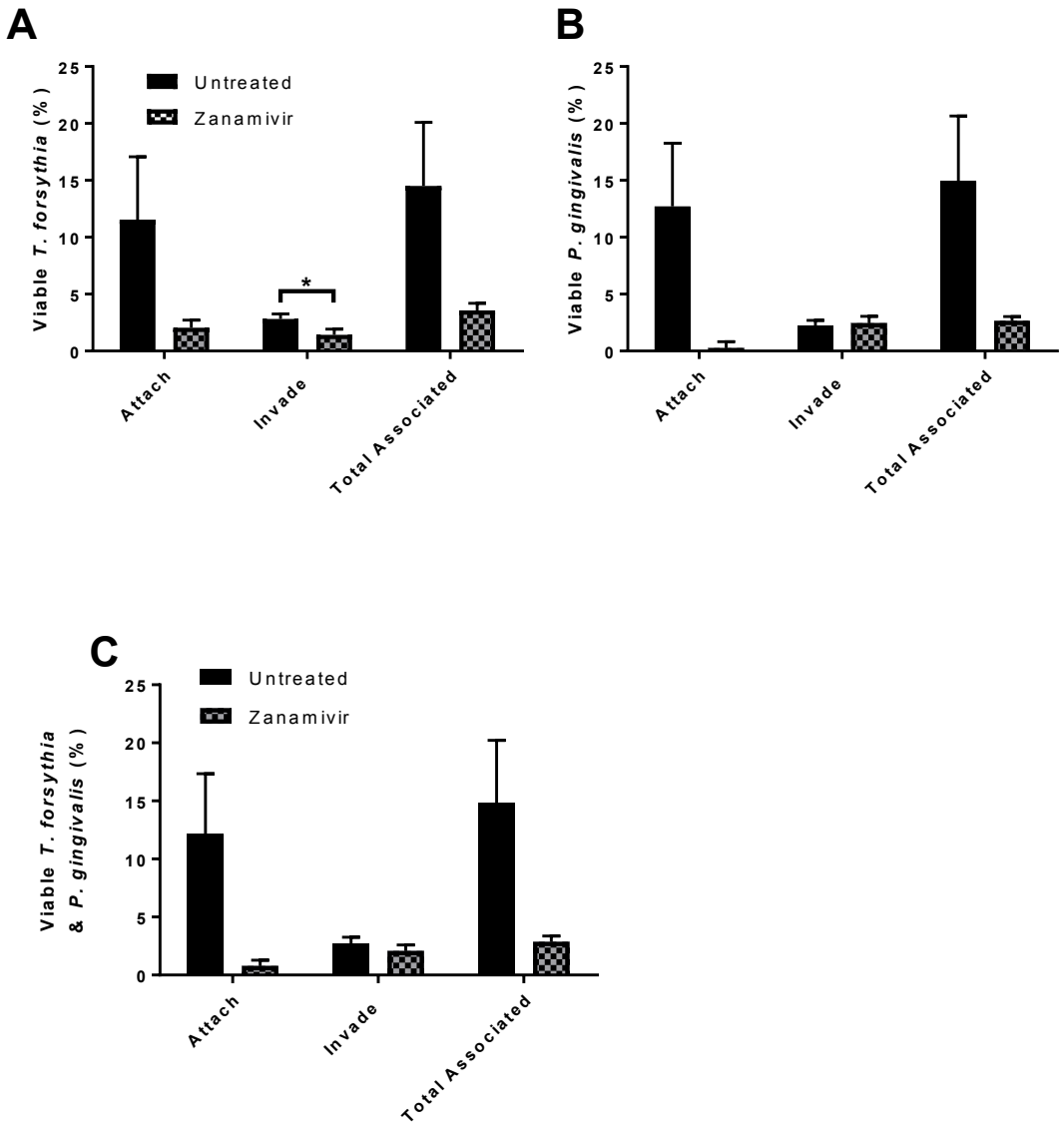

Supplemental figure S9. The effect of zanamivir on attachment and invasion of epithelial cells co-infected with *T. forsythia* and *P. gingivalis*.

Antibiotic protection assays were performed in the presence or absence of zanamivir with *T. forsythia* and *P. gingivalis A*) Level of *T. forsythia*-host cell association, B) Level of *P. gingivalis*-host cell association, or C) Level of both *T. forsythia* and *P. gingivalis*-host cell association. Bacterial attachment, invasion, and total association with host cells was normalised to the number of bacteria that were used to infect each condition that had survived the duration of the assay (the percentage of viable bacteria). Zanamivir= 10 mM zanamivir present during host cell exposure to bacteria. Data represent the mean from three experimental repeats, and each condition was repeated in triplicate during each experiment. Error bars=SEM. Significance determined by paired T-test, *p=<0.05.

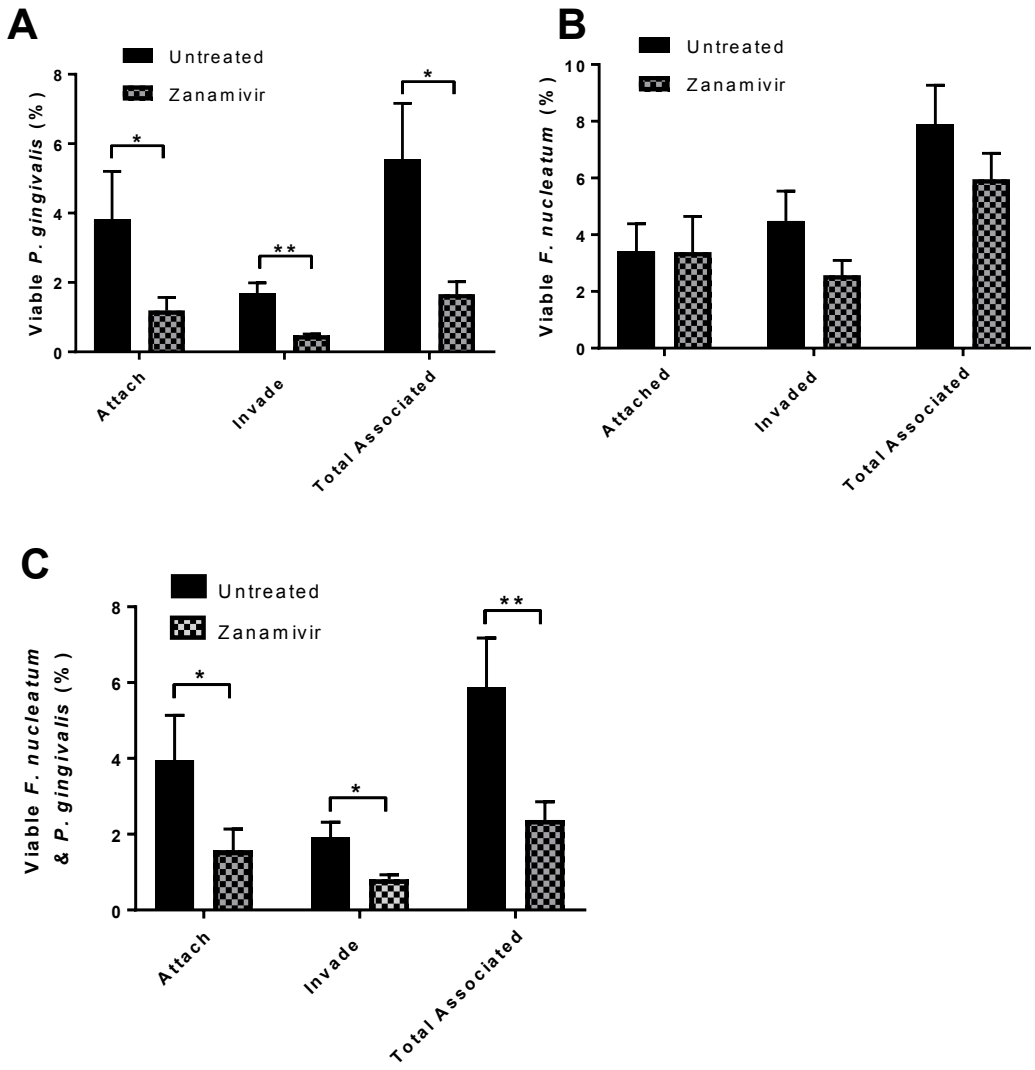

Supplemental figure S10. The Effect of Zanamivir on Attachment and Invasion of Epithelial Cells Co-infected with *P. gingivalis* and *F. nucleatum*.

Antibiotic protection assays were performed in the presence or absence of zanamivir with *T. forsythia* and *F. nucleatum* A) Level of *T. forsythia*-host cell association, B) Level of *F. nucleatum*-host cell association, or C) Level of both *P. gingivalis* and *F. nucleatum*-host cell association. Bacterial attachment, invasion, and total association with host cells was normalised to the number of bacteria that were used to infect each condition that had survived the duration of the assay (the percentage of viable bacteria). Zanamivir=10mM zanamivir present during host cell exposure to bacteria. Data represent the mean from three experimental repeats, and each condition was repeated in triplicate during each experiment. Error bars=SEM, Significance determined by paired T-test, *p=<0.05, **p=<0.01.

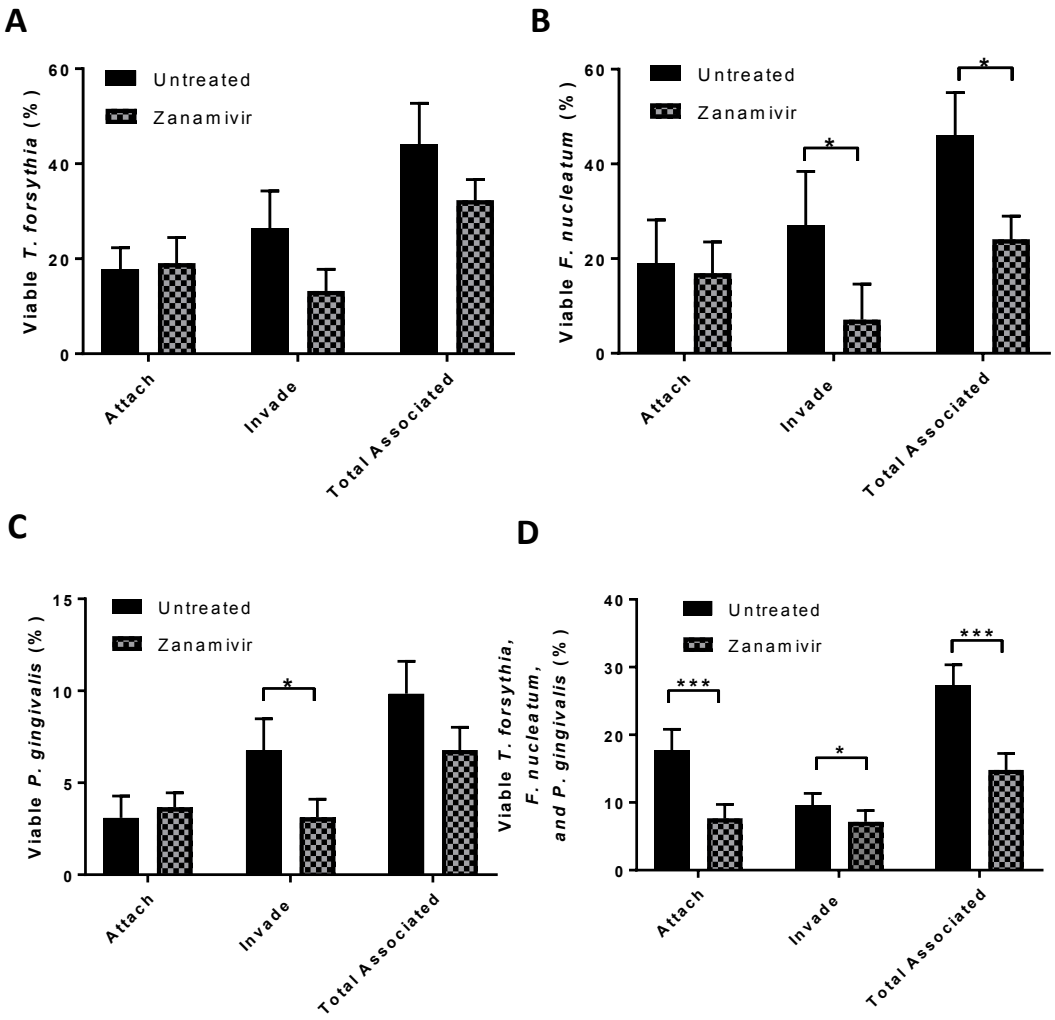

Supplemental figure S11. The effect of zanamivir on attachment and invasion of epithelial cells co-infected with *T. forsythia, F. nucleatum*, and *P. gingivalis*.

Antibiotic protection assays were performed in the presence or absence of zanamivir with *T. forsythia, F. nucleatum,* and *P. gingivalis.* A) *T. forsythia*-host cell association, B) *F. nucleatum*-host cell association, C) *P. gingivalis*-host cell association D) *T. forsythia, F. nucleatum,* and *P. gingivalis*-host cell association. Bacterial attachment, invasion, and total association with host cells was normalised to the number of bacteria that were used to infect each condition that had survived the duration of the assay (the percentage of viable bacteria). Zanamivir=10mM zanamivir present during host cell exposure to bacteria. Data represent the mean from three experimental repeats, and each condition was repeated in triplicate during each experiment. Error bars=SEM, Significance determined by paired T-test, *p=<0.05, **p=<0.01. ***p=<0.001.

Supplemental table 1. Composition of EPO glycans.

UHPLC Peak ID	% Area	ESI-LC/MS								
		Composition								
		Possible structure	Example Glycan cartoon	Hex (H)	HexNAc (N)	Fuc (F)	Neu5Ac (S)			potential sulphate or phosphate
							0 OAc	1 OAc	2 OAc	
1	0.16	Man4+P	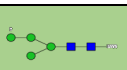	4	2	0	0	0	0	1
2	0.45	FMan4+P		4	2	1	0	0	0	1
3	1.23	Man5+P	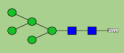	5	2	0	0	0	0	1
4	0.15	Man5+P		5	2	0	0	0	0	1
		FA2G2S2(Ac)2	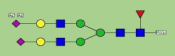	5	4	1	1	0	1	0
5	0.70	Man5+P		5	2	0	0	0	0	1
		FMan5+P	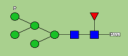	5	2	1	0	0	0	1
6	0.47	FMan5+P		5	2	1	0	0	0	1
		FA2G2S2(Ac)1	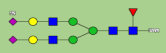	5	4	1	1	1	0	0
7	1.67	Man6+P	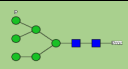	6	2	0	0	0	0	1
8,9	1.16	FA2G2S1		5	4	1	0	0	0	0
		Man6+P	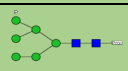	6	2	0	0	0	0	1
10,11	0.62	FMan6+P	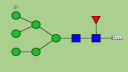	6	2	1	0	0	0	1
		Man6+P	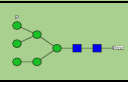	6	2	0	0	0	0	1

12	3.05	FA2G2S2	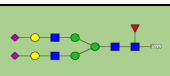	5	4	1	2	0	0	0
13	0.48	FA2G2S1S1(Ac)2	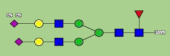	5	4	1	1	0	1	0
		FA3G3S2(Ac)1	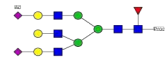	6	5	1	1	1	0	0
		FA2G2S2		5	4	1	2	0	0	0
		FA3G3S3(Ac)2	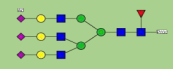	6	5	1	3	0	1	0
14,15	0.46	FA2G2S2	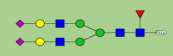	5	4	1	2	0	0	0
16	0.94	FA3G3S1	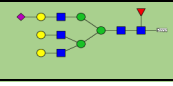	6	5	1	1	0	0	0

17	0.54	FA3G3S1	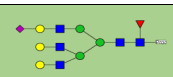	6	5	1	1	0	0	0
		FA4G4S3(Ac)2.	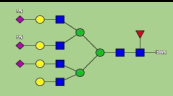	7	6	1	1	2	0	0
18	1.96	FA3G3S2	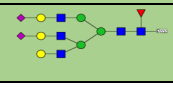	6	5	1	2	0	0	0
		A3G3S2(Ac)4	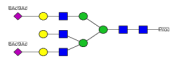	6	5	0	0	0	2	0
19	1.62	FA3G3S2	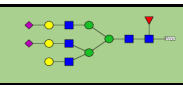	6	5	1	2	0	0	0
		A3G3S2(Ac)4	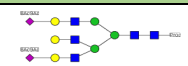	6	5	0	0	0	2	0
		FA4G4S3(Ac)2	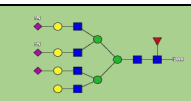	7	6	1	1	2	0	0
		FA4G4S4(Ac)2	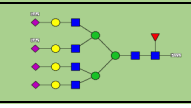	7	6	1	2	2	0	0

20	5.32	FA3G3S3	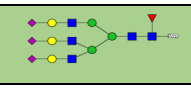	6	5	1	3	0	0	0
21	1.76	FA4G4S1 or FA3G3S1(LacNAc)1	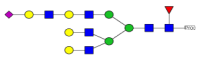	7	6	1	1	0	0	0
		FA3G3S3	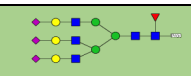	6	5	1	3	0	0	0
		FA4G4S4(Ac)2	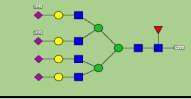	7	6	1	2	2	0	0
		FA4G4S3Ac	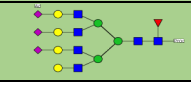	7	6	1	2	1	0	0

22	6.19	FA4G4S2 or FA3G3S2(LacNAc)1	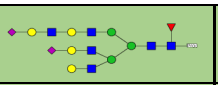	7	6	1	2	0	0	0
		FA4G4S4	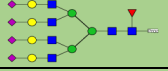	7	6	1	3	1	0	0
23	11.24	FA4G4S3 or FA3G3S3(LacNAc)1	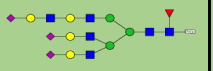	7	6	1	3	0	0	0
		FA4G4S4Ac	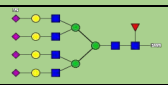	7	6	1	3	1	0	0
24	12.96	FA4G4S4	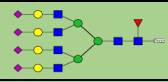	7	6	1	4	0	0	0
25,26	2.78	FA4G4S2(LacNac)1	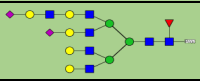	8	7	1	2	0	0	0
27	9.83	FA4G4S3(LacNac)1	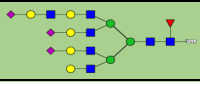	8	7	1	3	0	0	0

28	1.31	FA4G4S3(LacNac)1	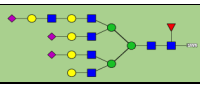	8	7	1	3	0	0	0
		FA4G4S3Ac2(LacNac)1	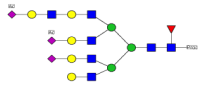	8	7	1	1	2	0	0
29	13.67	FA4G4S4(LacNac)1	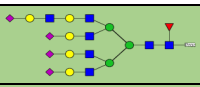	7	6	1	4	0	0	0
30	1.76	FA4G4S2(LacNac)2	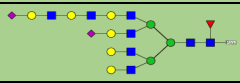	7	6	1	2	0	0	0
31	5.50	FA4G4S3(LacNAc)2	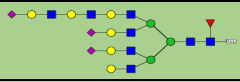	9	8	1	3	0	0	0
32	8.26	FA4G4S4(LacNAc)2	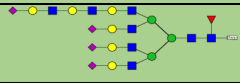	9	8	1	4	0	0	0
33	1.33	FA4G4S3(LacNAc)3	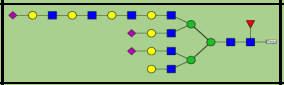	10	9	1	3	0	0	0
34	1.72	FA4G4S4(LacNac)3	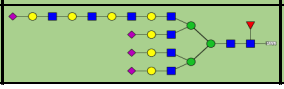	10	9	1	4	0	0	0